UNIVERSIDADE DE LISBOA

FACULDADE DE CIÊNCIAS

DEPARTAMENTO DE BIOLOGIA ANIMAL

Role of Wnt pathway on Rheumatoid Arthritis

Ana Henrique Baptista Daniel

Mestrado em Biologia Humana e Ambiente

Dissertação

2014

UNIVERSIDADE DE LISBOA

FACULDADE DE CIÊNCIAS

DEPARTAMENTO DE BIOLOGIA ANIMAL

Role of Wnt pathway on Rheumatoid Arthritis

Tese de Mestrado orientada por
Doutora Joana Caetano-Lopes - Department of orthopedic research, Children's Hospital Boston and Genetics department, Harvard Medical School, Boston, MA, USA
Professora Deodália Dias – Departamento de Biologia Animal da Faculdade de Ciências da Universidade de Lisboa

Ana Henrique Baptista Daniel

Mestrado em Biologia Humana e Ambiente

Dissertação

2014

Todas as afirmações efetuadas no presente documento são de exclusiva responsabilidade do seu autor, não cabendo qualquer responsabilidade à Faculdade de Ciências da Universidade de Lisboa pelos conteúdos nele apresentados.

As referências desta tese encontram-se formatadas de acordo com as regras da revista Nature.

Index

Agradecimentos

Em primeiro lugar gostaria de agradecer ao Professor João Eurico e à Doutora Helena Canhão pela oportunidade de realizar este trabalho na Unidade de Investigação em Reumatologia e fazer parte desta grande unidade. À Doutora Joana Lopes e á Professora Deodália Dias por me aceitarem sob a sua orientação ao longo deste ano e à Doutora Ana Maria Rodrigues por me integrar num projeto tão complexo e fascinante.

Agradeço a todas as pessoas com quem trabalhei que me ajudaram quando precisei e tornar o local de trabalho, mais animado e divertido, nomeadamente à Ana Lopes e às meninas da Histologia.

Gostaria de agradecer à Inês Perpétuo por tudo o que me ensinou durante este ano, tanto a nível profissional como pessoal, por me ajudares a ganhar responsabilidade e autonomia no trabalho. E claro, por todos os conselhos musicais e cinematográficos. “May the force be with you!”

Gostaria de agradecer ao meu “instrutor” Bruno Vidal, por tudo aquilo que me ensinou ao longo deste ano que me permitiu crescer enquanto cientista e pessoa e por todos os sábios conselhos, os sustos de morte e pela energia positiva transmitida.

Como não poderia faltar, quero agradecer às “ Melhores estagiárias” Rita Raposeiro, Rita Vieira e Joana de Sá, pela boa companhia no local de trabalho, companheirismo e amizade que formámos ao longo destes meses.

Às minhas grandes amigas, Marisa Rita, Fátima Mota e Filipa Cruz por me apoiarem sempre e por apesar da distância, no pouco tempo que estamos juntas tudo permanecer exatamente como antigamente. Julgo que não é preciso dizer mais nada, vocês sabem o quão importantes são para mim.

Gostaria de agradecer aos meus pais, especialmente à minha mãe por acreditar em mim e incentivar-me sempre a ir mais longe, sem ela nada disto seria possível.

E claro, ao resto da minha família e a todas as pessoas que fizeram parte da minha vida ao longo destes dois anos que de uma maneira ou de outra me ajudaram a chegar aqui e terminar mais uma fase importante da minha vida.

“ Love the life you live. Live the life you love “

Resumo

Artrite Reumatóide (AR) é uma doença crónica, inflamatória autoimune que afeta principalmente as articulações periféricas como as mãos e os pés, cuja causa é ainda ainda desconhecida. Esta doença tem uma incidência de cerca de 1% na população mundial, com maior prevalência no sexo feminino. As principais queixas por parte dos doentes são as articulações inchadas e dolorosas, rigidez matinal e fadiga. Para além destas queixas, esta doença é caracterizada a nível radiológico pela presença de erosões ósseas e destruição articular. Atualmente não existe um cura para esta doença, no entanto existem diversos tratamentos para melhor os sintomas e diminuir a progressão da AR: anti-inflamatórios não esteróides, corticosteróides, imunossupressores e mais recentemente drogas antirreumáticas biológicas, sendo estes últimos o tratamento mais inovador e melhorando significativamente a qualidade de vida destes doentes. Em doentes com artrite reumatóide ocorre infiltração do espaço sinovial entre as articulações por células do sistema autoimune que induzem a proliferação e ativação excessiva dos osteoclastos, que são as células responsáveis pela reabsorção óssea. Embora não sejam totalmente conhecidos os mecanismos que levam a este fenómeno, doentes com AR têm elevada reabsorção óssea que não é compensada pela formação óssea, devido a um comprometimento na proliferação e função dos osteoblastos, células responsáveis pela formação óssea. Ocorre assim um desequilíbrio que leva à perda de mineral óssea, sendo que muitos destes doentes sofrem de osteoporose secundária à inflamação. Ao nível dos osteoblastos, a via de sinalização Wnt controla a proliferação, ativação e funcionalidade destas células. Esta via pode ser inibida por diferentes proteínas, sendo as mais conhecidas DKK1, DKK2, SFRP1, SOST e WIF1. Segundo o que está descrito, a expressão dos inibidores da via de sinalização Wnt é induzida por fatores inflamatórios presentes nas membranas sinoviais de doentes com artrite reumatoide. Assim, a nossa hipótese é que a expressão destes inibidores está aumentada no osso de doentes com AR, o que leva a uma inibição dos osteoblastos.

Para isso, doentes com diagnóstico de AR segundo os critérios ACR/EULAR revistos em 2010 submetidos a artroplastia total da anca entre 2007 e 2014 no Serviço de Ortopedia do Hospital de Santa Maria, Centro Hospitalar Lisboa Norte, EPE foram selecionados de uma coorte armazenada no Biobanco-IMM (Centro Académico de Medicina de Lisboa). No Biobanco estavam armazenadas as cabeças femorais de doentes com AR submetidos próteses artroplastia total da anca (n=12) e ainda uma amostra de sangue. Como controlos, doentes com osteoartrose (OA) e osteoporose (OP) foram escolhidos da mesma coorte, com igual distribuição de sexo, idade e índice de massa corporal que os doentes com AR. De cada cabeça femoral foram recolhidos dois cilindros de diferente diâmetro, para testes mecânicos de compressão, colorações estruturais com hematoxilina e eosina, imunohistoquímica e ainda quantificação da expressão génica do osso trabecular. Realizámos ainda quantificação sérica de marcadores de remodelação óssea, P1NP marcador para a formação e CTX-I marcador para a reabsorção óssea.

Como modelo animal foram utilizados ratos Wistar com artrite induzida por adjuvante. Os valores do índice inflamatório, o peso e o perímetro do tornozelo foram registados ao longo dos 22 dias pós indução da doença e os animais foram eutanaziados ao vigésimo segundo dia. Após a eutanásia foi recolhida uma amostra

de sangue por punção cardíaca e os ossos longos e as vertebras foram também armazenados. Os níveis séricos dos marcadores de remodelação óssea (CTX-I e P1NP) foram quantificados. As vértebras foram recolhidas para histomorfometria, os fémures para testes mecânicos e quantificação do conteúdo mineral (por espectroscopia de energia dispersada por raios-X) e as tíbias para quantificação da expressão génica.

Ao comparar os doentes com AR e OA, não encontrámos quaisquer diferenças nos marcadores séricos CTX-I e P1NP, nos testes mecânicos de compressão nem ao nível da expressão génica do osso. Na comparação entre doentes com AR e OP, não encontrámos diferenças nos marcadores séricos de formação e reabsorção óssea, nem nos testes de compressão. No entanto, ao nível da expressão génica, os doentes com AR têm menor expressão de COL1A1 (gene que codifica o colagénio), RANKL (fator de diferenciação dos osteoclastos), WNT10B (proteína sinalizadora da via de sinalização Wnt), DKK1 e SFRP1 (inibidores da via de sinalização Wnt).

No modelo animal, Observámos que o marcador de reabsorção óssea (CTX-I) estava diminuídos nos ratos artríticos quando comparados com os saudáveis. Mais ainda, a percentagem de volume ósseo (BV/TV) estava diminuída nos ratos com artrite e a separação média entre as trabéculas (Tb.Sp) era maior nos ratos doentes em comparação com os saudáveis. O conteúdo de cálcio e fósforo estavam também diminuídos nos ratos com artrite o que se traduziu em piores propriedades biomecânicas. No entanto, não encontrámos qualquer diferença na expressão génica.

Os resultados obtidos com o estudo em amostras humanas não nos permite comprovar a hipótese postulada. Os resultados obtidos com o modelo animal sugerem que os ratos artríticos sofrem têm maior reabsorção óssea, o que se traduz em menor percentagem de volume ósseo, maior espaçamento médio entre as trabéculas e menor percentagem dos minerais constituintes da hidroxiapatite, cálcio e fósforo. Estas observações refletem-se em piores propriedades mecânicas no osso artrítico, sendo que este atinge o ponto em que perde a elasticidade e sofre a primeira fratura com uma menor força aplicada. Apesar de não conseguirmos confirmar ao nível da expressão génica que os inibidores da via Wnt estavam aumentados ao nível do osso em ratos com artrite, a expressão de genes ligados ao osteoblasto (como o RANKL e o LRP6) estava diminuída nos ratos com artrite.

Sendo assim, em amostras com artrite observamos que existe reabsorção óssea aumentada, e que existe um comprometimento nos osteoblastos que não lhes permite formar osso e assim compensar a excessiva atividade dos osteoclastos. Isto leva à perda de massa óssea e à perda de massa óssea o que leva a uma maior suscetibilidade a fraturas de baixa intensidade características de doentes osteoporóticos. Infelizmente não conseguimos comprovar a nossa hipótese de que os doentes com artrite têm um comprometimento nos osteoblastos devido à expressão de inibidores da via Wnt no osso.

No futuro, serão necessários mais estudos para tentar compreender que mecanismos levam ao comprometimento dos osteoblastos e a íntima relação entre o sistema imune e o tecido ósseo.

Abstract

Rheumatoid Arthritis (RA) is a chronic inflammatory autoimmune disease that affects the peripheral joints. It is characterized by infiltration of the synovial membrane by immune cells and by bone erosions. These patients have increased bone resorption with low bone formation, leading to loss of bone mass. The low bone formation rate observed in arthritis is due to impairment of osteoblast activity, most likely to a deregulation of the canonical Wnt pathway. Osteoblast proliferation and activity is regulated by the Wnt signaling pathway which itself is controlled by several inhihbitors like Dickkopf proteins and sclerostin. Wnt inhibitors are highly expressed on the synovial membrane of RA patients. Our hypothesis is that the high expression of Wnt inhibitors at the bone level leads to osteoblast impairment in RA.

To test our hypothesis we collected the femoral heads of 12 RA patients as well as serum samples. We used gender and age matched osteoarthritis (OA) and osteoporosis (OP) patients as controls. Quantification of serum bone turnover markers, mechanical compressive tests, and trabecular gene expression was performed. We have also used Wistar rats with adjuvant induced arthritis. Rats were euthanized at 22 days post-disease induction. Blood samples and bones were collected, to measure of bone turnover markers, perform histomorphometry, three-point bending, energy-dispersive X-ray spectroscopy and bone gene expression.

No differences were found on the comparison of RA and OA patients. No differences were found between RA and OP patients, except that RA patients have decreased expression lower osteoblast gene expression. Arthritic rats have, higher CTX-I levels, lower BV/TV and Tb.Sp., lower Ca and P percentage, and worst mechanical properties than healthy controls. No differences were found on gene expression.

Concluding, arthritis-affected bones have an impairment of osteoblasts and consequently worst bone quality, mechanical properties and less mineral content.

Introduction

Rheumatoid Arthritis

Rheumatoid arthritis (RA) is a chronic inflammatory disease, characterized by inflammation of the joint lining tissues (synovia)[1]. The prevalence of the disease on the world population is around 1% with a higher incidence on women, approximately twice than in men[2]. The symptoms of the disease include chronic inflammation of the synovial joints, progressive destruction of cartilage and bone, severe joint pain and life-long disability[3]. In the synovial membrane a proliferation of cells and infiltration of inflammatory cells occurs into the joint space[4] resulting in the formation of a tissue named “pannus” around the surfaces of the articular cartilage and bone[1]. During chronic inflammation, the balance between bone formation and resorption is skewed towards osteoclast (OC)-mediated bone resorption. Unlike other rheumatic diseases, in sites adjacent to inflamed areas, within the bone of these patients there is little evidence of new bone formation suggesting that the inflammation impairs osteoblast (OB) activity. In fact, fully differentiated osteoblasts are rarely seen in arthritic bone erosions indicating that there is no major bone formation taking place in these lesions[5,4]. Therefore, osteoblast activity does not compensate the excessive bone resorption[4]. This failure to compensate occurs not only near the joints but also at non-inflamed skeletal sites thereby contributing to the development of secondary osteoporosis (OP)[6] and a consequence decreased bone mineral density, systemic bone fragility and fractures[7,8].

RA and immune system

Activation of immune cells is a requirement for defense of the host against pathogens, however an increased activation of immune cells can result in tissue damage[9]. In RA joints, the over-expression of Receptor activated of Nuclear Factor- κ B ligand (RANKL) due to T-cells and synovial fibroblasts activation in the joints, induces osteoclast differentiation leading to an increase of osteoclast activity and consequently to pathological bone destruction[10,4]. As demonstrated by Lubberts and colleagues, in collagen-induced arthritis (CIA) mice, the number of cells expressing ligands and receptors involved in osteoclast differentiation is increased[11]. For example, in the pannus tissue from active RA patients, RANK and RANKL, which are required for osteoclast differentiation, are both increased as arthritis progresses and, in areas of abundant RANK expressing cells, tartrate-resistant acid phosphatase (TRAP) positive multinucleated osteoclasts are also present[11,12].

Animal models for RA studies

There are several animal models of arthritis and the most common ones are rodents, like rat and mouse. Animal models for arthritis can be divided in two major groups: the induced and the spontaneous, being the first one more advantageous because we know what is the triggering mechanism of arthritis which gives rise to an immune response[13]. Animal models allow us to assess the early phase of arthritis and understand how disease induction occurs. One of the aims of using animal models is to understand RA pathology by the study of the early phase of disease, or the induction phase, in which symptoms are still not present, which is very difficult in RA patients as they already present symptoms when are diagnosed[13]. Besides that, several animal

models are also used to test anti-arthritic drugs which are either under preclinical or clinical investigation or are currently used to treat this disease[14,15].

Adjuvant-induced-arthritis (AIA) Wistar model

Wistar rats belong to the *Rattus norvegicus* species and were first rat developed to serve as a model organism. Another important point to consider is the sexual maturation of the animals, which is achieved at eight-nine weeks, corresponding to a weight of 200-250g.

The adjuvant-induced arthritis model was originally used to study the eicosanoid pathway and test non-steiroidal anti-inflammatory drugs (NSAIDS). Actually is frequently associated with DMARDs research (Disease-modifying antirheumatic drugs), sintetic or natural[16].

The AIA model is an induction model of arthritis, consisting of inoculation of a pathogen by intradermal injection, at the base of the tail[17]. This is an acute model of the disease, and disease onset occurs 10 days after the induction[17,16]. The disease reaches a plateau of inflammation around the 19th day of disease. As the prevalence of RA is higher in females, the majority of arthritis studies use female rats for the AIA model.

As any other model, AIA rat has similarities and differences comparing with human RA. The main similarities are the symmetrical joint involvement, peripheral joints affected, persistent joint inflammation, synovial hyperplasia, inflammatory cell infiltration and marginal erosions. The main differences are the rapid onset of highly erosive polyarthritis, involvement of axial skeleton, no rheumatoid factor, gastrointestinal, genitourinary and skin involvement, bony ankylosis and extra-articular manifestations not typical of RA[17]. However the major advantage of using this model is that AIA Wistar rats arthritis resembles human RA at the level of genetic linkage and the immune response cells hence this rat model is also usually used to test several drugs against RA[13].

Bone

Bone is a dynamic tissue that undergoes constant adjustment to preserve and achieve the shape and structure of the skeleton, maintain structural integrity and regulate mineral homeostasis[18,19].

Bone Microstructure

At the microscopic level, bone is composed of a cortical and a trabecular portion. Cortical bone represents 80% of skeletal bone and is dense and compact with a lower turnover ratio. This type of bone constitutes the outer part of all bones, providing mechanical strength and protection[20]. The trabecular bone only composes 20% of the whole skeleton, and is found inside the long bones surrounded by cortical bone[21]. This kind of bone has a very porous structure, is much more elastic, and has a higher turnover rate. It provides mechanical support to bones, such as the vertebrae and femurs, and has an important role on calcium homeostasis[20,]. Inside the bone we can find the bone marrow, between trabecular porous and surrounded by cortical bone[22]. Both trabecular and cortical bone are composed of osteons, but cortical osteons have concentric layers of bone, while trabecular bone has parallel fibbers of collagen and hydroxyapatite crystals[20].

Bone molecular structure

Bone is a heterogeneous composite material composed by an inorganic or mineral phase of hydroxyapatite ($Ca_{10}(PO_4)_6(OH)_2$) crystals, and an organic phase of collagen and noncollagenous proteins, lipids and water[23]. These components provide hardness and viscoelasticity to bone tissue[24].

Inorganic component

Hydroxyapatite is the major component of the mineral phase of bone[23]. These crystals are formed by calcium and phosphorus present in the bloodstream and both minerals suffer several transformations until their incorporation into the hydroxyapatite crystals. Vitamin D plays an important role on the correct organization of crystals on bone due to its involvement in the decarboxylation of osteocalcin (OCN)[25], a protein that is responsible for correct deposition of calcium molecules between the phosphorus[26]. The hydroxyapatite crystals are then aligned with the collagen proteins to form fibrils and fibers[24].

Organic component

The organic component of bone is composed mostly by collagen type I (90%) and non-collagenous proteins[21]. Collagen type I is synthesized by osteoblasts and is deposited in parallel or concentric layers (lamellar bone)[21]. There are several non-collagenous proteins on bone, although the most important ones are OCN and alkaline phosphatase (ALP). The first one is involved in calcium binding and hydroxyapatite stabilization, and the second one is an enzyme responsible for pyrophosphate (PPi) hydrolysis to generate inorganic phosphate (Pi) which is crucial for the formation of hydroxyapatite[20,27].

Bone cells structure

When a damage or microfracture occurs in the bone, the responsible cells come into action and those are osteoblasts, osteoclasts and osteocytes[28,29]. These three types of cells form the basic multicellular unit (BMU).

Osteoblasts (OB) and the Wnt pathway

Osteoblasts have two important functions on bone: they are responsible for bone formation and they modulate osteoclast differentiation by producing RANKL[1] and macrophage colony-stimulating factor (M-CSF) [30,31]. Osteoblasts also secrete osteoprotegerin (OPG), a decoy of receptor for RANKL, which in turn inhibits osteoclast formation[32,28,18]. Osteoblasts are derived from mesenchymal stem cells, which can also give rise to chondrocytes or adipocytes, depending on growth factors, hormonal regulators and transcriptional factors involved[6,33,28]. In the case of osteoblasts, the major osteogenic factors are Runt-related transcription factor 2 (Runx2), osterix (Osx) and β-catenin (Fig.1) [34,31].

Runx2 is expressed at early phases of osteoblastogenesis and is responsible for mesenchymal cell commitment. This transcription factor is responsible for the expression of Osx, OCN and type I collagen (Col1a1)[31]. Osx is expressed at the final steps of this process, having an important role in the segregation of osteoblasts from osteochondrogenitors and also inducing the expression of OCN and Col1a1[34,31].

When these cells achieve the mature state they also express ALP and OCN, both involved in matrix production[28]. OCN (after carboxylation) attracts calcium ions and incorporates them into hydroxyapatite crystals, consequently stopping bone formation[35,36,37]. When osteoblasts lose their synthesis capacity they either become lining cells, osteocytes or they die by apoptosis (Fig.1)[4,33].

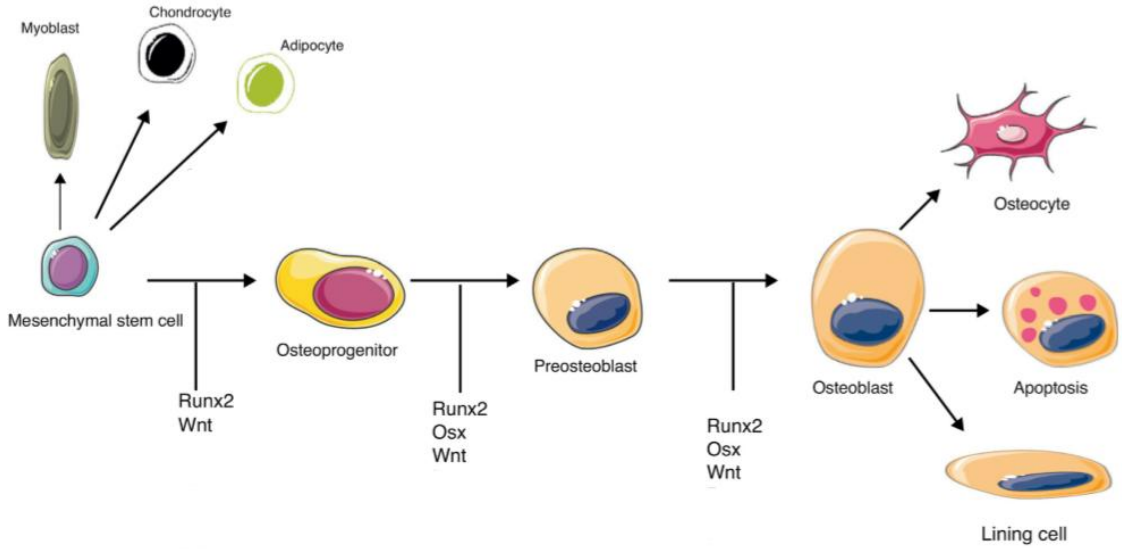

Figure 1 Pathways that are essentialfor osteoblast differentiation and activation. Mesenchymal stem cells are able to give rise to myoblasts, chondrocytes, or adipocytes when the Wnt pathway is not activated. On the contrary, when this pathway is active, osteoblast commitment and differentiation occurs. During osteoblastogenesis, Runx2 and Osx are also essential factors. At the end of osteoblasts life, they become osteocytes, lining cells or die. Adapted from [4]. MyoD - myogenic differentiation; Sox9 - SRY (sex determining region Y)-box 9; PPARy - peroxisome proliferator-activated receptor y; Runx2 - runt-related transcription factor 2; Osx – osterix.

Osteoblast commitment and differentiation is strongly dependent on the Wnt/β-catenin signaling (canonical Wnt pathway; Fig.2)[28]. Canonical Wnt pathway determines the fate of mesenchymal stem cells[38].

Briefly, in the absence of WNT proteins, GSK-3β phosphorilates β-catenin, which is degraded and the osteoblast signaling cascade is blocked, so the stem cells become chondrocytes or adipocytes[30,38]. When Wnt proteins are present, they bind to the frizzled receptor and a low-density lipoprotein receptor-related protein (LPR5/LRP6), activating the signaling cascade[1]. These receptors transduce a signal to a complex formed by dishevelled protein (Dsh), glycogen synthase kinase-3β (GSK-3β), axin and adenomatous poluplosis coli (APC), which promotes the phosphorilation and inhibition of GSK-3β[39,40]. As result, β-catenin can accumulate in the cytoplasm and translocate to the nucleus where the expression of the transcription factors T-cell factor/lymphoid enhancer factor (TCF/LEF) and consequently the expression of osteoblast related genes and OPG[40]. The activation of the Wnt signaling pathway promotes stem cell differentiation into ostoblasts. The increase of this signaling pathway also leads to inhibition of osteoclastogenesis by inducing the expression of OPG by osteoblasts[39,30].

When the Wnt pathway is activated, osteoblast differentiation occurs, but in the presence of antagonists like DKK1, secreted frizzled related proteins (sFRPs), SOST

or Wnt inhinitory factor-I (Wif-I), the signaling is inhibited[38,40]. DKK and SOST are the most well studied endogenous Wnt inhibitors.

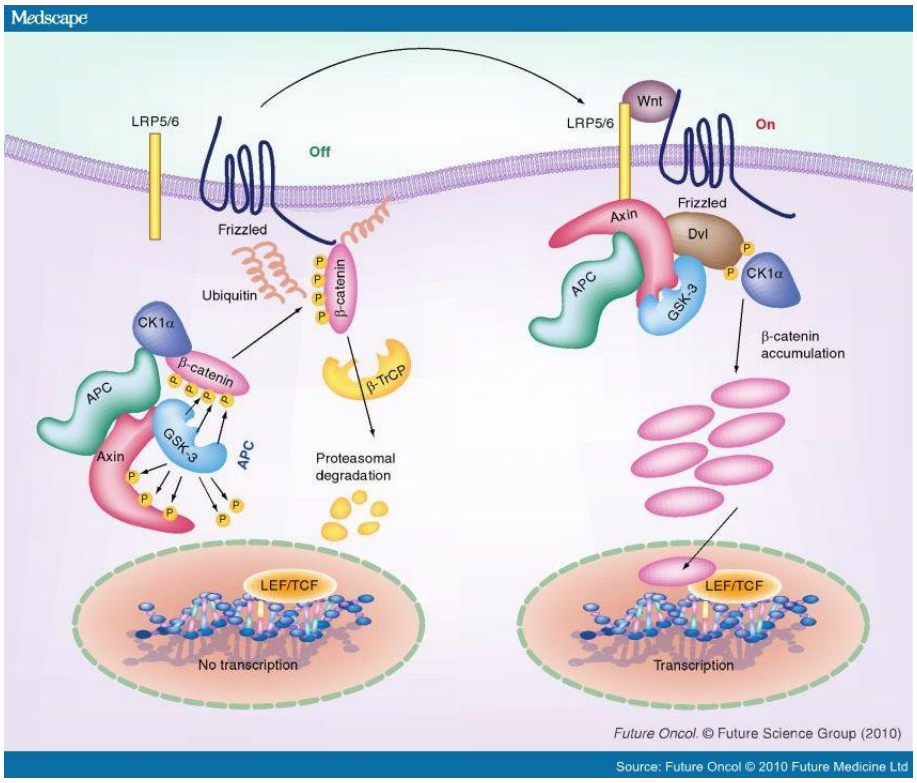

Figure 2 Wnt pathway[41]. On the left, in the absence of Wnt proteins, GSK-3β phosphorylates β-catenin, so that it undergoes proteossomal degradation. On the right, Wnt proteins bind to the receptor LRP5/LRP6, inhibiting GSK-3β and allowing the accumulation of β-catenin which translocates to the nucleus and induces the expression of LEF/TCF. LRP5 - low-density lipoprotein receptor-related protein 5; LRP6 - low-density lipoprotein receptor-related protein 6; Dsh - dishevelled protein; APC - adenomatous poliposis coli, GSK-3β - glycogen synthase kinase-3β; TCF - T-cell factor; LEF - lymphoid enhancer factor.

DKK1 is produced by osteocytes and osteoblasts and binds to LRP6 with high affinity, and to the Kremen[28]. Kremen2, DKK1 and LRP6 form a complex that promotes removal of the Wnt receptor from the plasma membrane by endocytosis[40,42]. DKK1 expression is also induced by TNF[9]. DKK2 acts like an agonist or an antagonist of LRP6 depending of the presence of Kremen2. When Kremen2 is absent, the Wnt signaling pathway is activated, but in the presence of Kremen2 it is inhibited[28].

Sclerostin is the product of the SOST gene, which mainly expressed by osteocytes[43]. Moreover, this protein is secreted by osteocytes in response to a mechanical force, arresting bone formation[44]. Sclerostin binds to the LRP5/6 co-receptor, so β-catenin is sequestered and degraded, therefore sclerostin acts as a Wnt inhibitor[28].

Osteocytes (OCY)

Osteocytes are osteoblasts that become entrapped into the bone matrix. This is the most abundant cell type on bone and they are found in lacunae on the mineralized matrix[19]. They communicate with each other and with other cells such as osteoblasts and osteoclast progenitors through an extensive system of canaliculi[33,45]. Osteocytes are able to sense bone microfractures, thereby signalling the need for repair[46].

Osteocytes can also control mineral homeostasis[45]. The death of osteocytes by apoptosis signals the presence of damage on its location and is considered the initiation of targeted remodeling[28,19]. In recent years the role of osteocytes has been appreciated in the control of bone mass through the discovery of SOST and DKK1, produced mainly by these cells. Both SOST and DKK1 play a critical role in the inhibition of bone formation by inhibiting with the Wnt pathway[46].

Osteoclasts (OC)

Osteoclasts are multinucleated giant cells formed by the fusion of mononuclear progenitors from monocyte-macrophage lineage cells[32,30]. These cells are specialized in the removal of mineralized bone matrix[30]. Differentiation of osteoclasts occurs in response to M-CSF and RANKL produced mainly by osteoblasts but is blocked by OPG, also produced by osteoblasts[18,30].

Bone remodeling process

The remodeling process occurs throughout life and has a pivotal role in the maintenance of the mechanical integrity of the skeleton, repair of fractures and mineral homeostasis[47]. The remodeling process consists of five phases:

1. Activation

The first phase involves the detection of a signal, such as structural damage, leading to recruitment and activation of osteoclasts precursors from the circulation[18,21].

2. Resorption

Osteoblasts respond to signals generated by osteocytes and the expression of OPG is reduced with an increase of M-CSF and RANKL production to promote osteoclast formation and activation[20]. Osteoblasts also produce matrix metalloproteinases (MMPs) which degrade the unmineralized osteoid facilitating osteoclast attachment[33]. When they attach an isolated microenvironment known as the “sealing zone” is created. The osteoclast secretes hydrogen ions to the sealing zone creating an acidic environment allowing the dissolution of the mineralized matrix. Then, a set of collagenolytic enzymes, in particular cathepsin K, have the low pH necessary to degrade the organic bone matrix[18,48].

3. Reversal

After resorption the Howship’s lacunae remains covered with undigested demineralized collagen matrix, and the cells responsible for the removal of matrix debris (osteomacs - bone macrophages) act during this phase[18]. These cells may play a role on the receiving or producing signals that allow the transition from bone resorption to bone formation[21].

4. Formation

Mechanical stimulation and parathyroid hormone (PTH) can lead to bone formation via osteocyte signals. Under resting conditions, osteocytes secrete sclerostin that binds to LRP5/6 and impairs Wnt signaling, an inducer of bone formation[18]. Mechanical strain and PTH inhibit osteocyte expression of sclerostin, removing the inhibition of Wnt signaling and allowing Wnt-directed bone formation, so osteoblast progenitors return to resorption lacunae, differentiate into osteoblasts and form bone. Collagen type I is the

primary organic component of bone, and non-collagenous proteins add the remaining organic material. Ultimately, hydroxyapatite is incorporated into this newly deposited osteon[24].

5. Termination

The termination signals to cease the remodeling process are still unknown, although we believe that when osteoblasts become embedded in the mineralized matrix and differentiate into osteocytes, their sclerostin expression increases bringing the end of the remodeling cycle[18]. At the end of the remodeling process the quantity of resorbed bone should be equal to the total of formed bone[21].

Bone turnover markers

Bone turnover markers are biochemical products usually measured in blood or urine that allow the quantification of the bone's metabolic activity[49,50]. These molecules are thought to have no function in controlling skeletal metabolism and they are classified as bone formation or bone resorption markers[50]. Total OCN, ALP bone isoenzyme and the C and N-propeptide of type I collagen (P1NP) are examples of the most used bone formation markers, while type I collagen cross-links (pyridinoline-PYD and deoxypyridinoline-DPD), N-terminal cross link telopeptide of type I collagen (NTX) and C-terminal cross-link telopeptide of type I collagen (CTX-I) are the most common markers of bone resorption[51]. P1NP released to circulation is a product of enzyme cleavage of procollagen type I during bone matrix formation, while CTX-I is released during cathepsin K activity during bone resorption[50].

Objective

In RA, a trigger leads to immune system hyper-activation. As the immune system and bone are connected, this triggers leads to an excess of bone resorption by osteoclasts, which in normal conditions is compensated by the formation of new bone carried out by osteoblasts. However, pro-inflammatory cytokines disrupt not only the OC-OB communication but also the Wnt signalling pathway. The upregulation of Wnt antagonists like DKK1 has been implicated in the suppression of osteoblast activity during inflammation-induced bone loss[5,42]. Reduced Wnt activation and an increase in osteoclast activity leads to an increase in osteoclast-mediated bone resorption in RA[52].

Therefore, our hypothesis is that Wnt inhibitors are upregulated on bone leading to osteoblast loss of function. Our goal is to study bone at several levels, beginning on the gene expression of osteoblast markers and Wnt related genes and also access the bone turnover ratio and determine the bone quality and microstructure.

Material and Methods

Patients

This was a nested case study from a cohort of 1035 consecutive patients undergoing total hip replacement surgery at Lisbon Academic Medical Centre, with bone samples stored in a biobank (Biobanco-IMM) in Lisbon. Patients who were diagnosed with RA according to the 2010 ACR/EULAR revised classification[53] and submitted to total hip replacement surgery between 2007 and 2014 were selected from the biobank collection and included in this study. Patients were excluded if other causes of secondary OP were present, such as malignancies, untreated thyroid disease, terminal renal disease or hypogonadism and if they were under anti-osteoporotic treatments.

Two other groups undergoing hip arthroplasty due to hip fragility fracture or Osteoarthritis (OA), matched to gender, age and body mass index (BMI), and without any secondary causes for Osteoporosis (OP), were selected from the biobank to be used as control groups.

All patients were asked to complete a clinical questionnaire at the time of surgery in order to assess clinical risk factors associated with OP, such as age, gender, BMI, prior fragility fracture, family history of hip fracture, long-term use of oral corticosteroids ($\geq$3months), current smoking and alcohol intake ($\geq$3 units/day) and past and current medication. Four days after the surgery, Bone Mineral Density (BMD) of the contralateral hip was measured by dual X-absorptiometry (DXA) scan using a Lunar Prodigy densitometer (Lunar Prodigy, GE Healthcare at the Rheumatology and Bone Metabolic Diseases Department of Hospital de Santa Maria. For RA patients, disease duration, age at disease onset, rheumatoid factor, C-reactive protein (CRP), disease activity score (DAS28 ESR3V), presence of erosions, and RA therapy were also assessed.

Serum samples were collected from patients at the time of surgery for biomarkers measurement. The femoral heads removed from the patients were collected and processed. From the femoral epiphysis two cylinders were drilled, one used for mechanical tests (15 mm diameter), while the other (18 mm diameter) was cut and used for immunohistochemistry. Small pieces of trabecular bone were collected and frozen for gene expression study.

Written informed consent was obtained from all patients. This study was conducted in accordance with the regulations governing clinical trials such as the Declaration of Hensinki, as amended in Fortaleza (2013), and was approved by the Hospital de Santa Maria Ethics Committee.

Rat model

Wistar AIA rats (N = 21) were purchased from Charles River Laboratories International. Eight-week-old females weighing 200–230 g were maintained under specific pathogen free (SPF) conditions and all experiments were approved by the Animal User and Ethical Committees at Instituto de Medicina Molecular, according to the Portuguese law and the European recommendations.

At Charles River, nine animals were inoculated under isoflurane anesthesia by subcutaneous injection of complete Freund's adjuvant (CFA) containing *Mycobacterium butyricum* in the right paw, which causes a profound systemic

inflammatory reaction resulting in severe joint swelling and destruction[54,17]. As controls, 12 healthy Wistar rats were used.

The inflammatory score, ankle perimeter and body weight were measured during the study period every other day. Inflammatory signs were evaluated by scoring each joint in a scale of 0-3 (0 - absence of any sign, 1 - erythema, 2 - erythema and swelling, 3 - deformity and functional impairment). The total score of each animal was defined as the sum of the partial scores of each affected joint. Rats were sacrificed after 22 days of disease evolution when they were 3 months of age.

At the time of sacrifice vertebrae and long bones, such as femur and tibia, were collected for histological evaluation, RNA extraction and three point bending test. Blood samples were collected by cardiac puncture for bone turnover markers assessment.

Bone turnover markers measurements

Carboxy-terminal cross-linked telopeptides of type I collagen (CTX-I) and amino-terminal propeptides of type I procollagen (P1NP) were measured by enzyme linked immunosorbent assay (ELISA) in human and rat serum. Human CTX-I and human P1NP ELISA kits (SunRed Biological Technology) and rat (Immunodiagnostic Systems Ltd) were used according to the manufacturer's instructions and read in a Tecan Infinite 200 PRO (Tecan Group).

Histological techniques

Sample processing

Trabecular bone from femoral epiphysis was fixed in formaldehyde 10% (VWR) for 7 days, decalcified in Ethylenediaminetetraacetic acid(EDTA, Promega) 10% for 14 days, dehydrated in increased alcohol concentrations (70%, 96%,100%, 24 hours each) and embedded in paraffin. Five sections with 5µm thickness were cut in a microtome (Leica RM2145, Leica). Before hematoxylin and eosin staining or immunohistochemistry the samples deparaffinized with xylene and hydrated with decreasing alcohol solutions (100%, 96%, 70%), ten minutes each.

Hematoxilyn and eosin staining

Hematoxylin and eosin staining (H&E) is one of the principal stains in histology. It is the most widely used stain in medical diagnosis, allowing the differentiation between cytoplasm (pink) and nucleus (blue) providing a good staining for standard analysis[55]. Hematoxilyn has a basic pH with affinity to acid structures, while eosin has an acid pH with affinity to basic structures.

The staining was performed with hematoxilyn (Bio-Optica) for five minutes, and five minutes of warm running water for hematoxilyn oxidation. The samples were then immersed in alcohol 70% before the counterstaining in alcoholic eosin (Thermo Scientific). Slides were dehydrated with increasing alcohol solutions (70%, 96%, 100%) for thirty seconds each, and after fifteen minutes in Xylene were mounted with Quick-D mounting medium (Klinipath).

Immunohistochemistry of femoral epiphysis

Immunohistochemistry is a technique based in the principle of antigen-antibody binding that allows the identification of proteins of interest in the tissue samples[56].

As our samples were embedded with paraffin, the antigen sites were cover so we performed antigen retrieval to uncover the epitopes and restore the immunoreactivity. Antigenic retrieval was performed with Proteinase K (Sigma-Aldrich), incubating for twenty minutes at 37ºC and then 10 minutes at room temperature. Endogenous peroxidase was blocked with a solution of 1.5 % hydrogen peroxide in methanol (VWR) for 15 minutes at room temperature. Total proteins were blocked with PBS/BSA 1% (Fluka) for twenty minutes. Samples were incubated with primary antibody for one hour at room temperature. An envision polymer with horseradish peroxidise ((1µg/mL, HRP, Dako) was used as a secondary antibody. All washes were performed with PBS/Triton (Sigma-Aldrich) or distilled water. At the end, 3, 3'-diaminobenzidine (DAB, Dako) was used as development solution. Slides were counterstained with Harris hematoxylin (Bio-Optica,), dehydrated with increasing alcohol solutions (70%, 96%, 100%) for thirty seconds each, fifteen minutes in Xylene and mounted Quick-D mounting medium. Negative control follows the same protocol except the primary antibody staining.
The antibodies used were anti-DKK1 (ab109416, 1:500), anti-osteocalcin (ab13420, 10µg/ml) and anti-SOST (ab63097, 1:50), all from AbCam.
Slides were observed at a brightfield microscope (Leica DM2500, Leica) and photographed with camera CCD (Leica). DKK1 samples were scored with 1 (0-25% staining osteocytes), 2 (26-50% staining osteocytes), 3 (51-75% staining osteocytes) or 4 (76-100% staining osteocytes). Slides stained with osteocalcin were scored with 1 (sample without osteoblasts), 2 (sample with less of 50% of labelled osteoblasts) and 3 (sample with more than 50% of labelled osteoblasts). SOST was scored with 1 (0-25% staining osteocytes), 2 (26-75% staining osteocytes) and 3 (76-100% staining osteocytes).

Histomorphometry of rat vertebrae

Histomorphometry is a technique used for the quantitative study of the microscopic organization and structure of a tissue, such as bone, in 2D allowing the extrapolation for 3D results. Microarchitecture can be assessed by static parameters, such as trabecular thickness (Tb. Th) and trabecular separation (Tb.Sp). These architectural parameters are related to the bone volume fraction (BV/TV) value. BV/TV value is the percentage of area occupied by calcified bone in relation to the total sample area. Tb.Th is the medium distance across individual trabeculae and Tb.Sp is the medium distance between trabeculae of our region of interest[57].

We used the L4 vertebrae to study bone fragility by histomorhometry. The samples went through five phases: fixation with ethanol 70% for 7 days, dehydration with increasing ethanol concentration from 96% to 100% during two days each, clearing with xylene for 4 hours, impregnation with methyl methacrylate (Sigma-Aldrich) for a minimum of 72 hours, and embedded in a solution of dimethylaniline 2% (Merck) in methyl methacrylate (Sigma-Aldrich). Dimethylaniline was used as catalyst to promote the polymerization. During these five steps the samples were maintained at 4ºC.

After the polymerization, the samples were cut in a microtome (Leica) with a tungsten blade (Leica), enabling the cut of calcified bone samples. We cut three sections with 5µm of thickness. Slides coated with gelatine chrome alum (Panreac) together with polyethylene film were used to keep the sample attached. Samples were then stained with aniline blue (VWR). Briefly, the slides were immersed in ponceau fuchsin (Sigma-Aldrich) for two minutes, washed with acetic water 1% (Sigma-Aldrich) and distilled water. Thereafter slides were incubated with aniline blue 0.2% (Sigma-

Aldrich) for fifteen minutes. Lastly slides were washed with distilled water and then dehydrated with increasing ethanol solutions (70%, 96%, and 100%), immersed in xylene and mounted with Quick-D mounting medium. The entire preparations were observed with Leica DM2500, objective 1.25x and photographed with camera CCD (Leica). Samples were than analysed using Bone J plugin[58] (England) of Image J software[59,60] (NIH). For each sample the following structural parameters were evaluated: Bone volume (%) (BV/TV), Trabecular thickness (Tb.Th) (µm) and Trabecular separation (Tb.Sp.) (µm).

Energy-dispersive X-ray spectroscopy

EDX consists in the emission of a solid sample with an electron beam in order to obtain a localized chemical analysis. This method is based on the difference of energy caused by the excitation of an electron that causes its injection to the next orbital of the atom and an electron of an outer orbital of higher-energy then fills the hole. The difference in energy between the higher-energy orbital and the lower energy orbital is released in the form of an X-ray. This technique was used in order to quantify the calcium and phosphorus concentration in the rat bone samples.

After rat femurs collection, samples were dried for 46 hours, with a multipurpose ice condenser (ModulyoD-230, Thermo Savant) operated at a nominal temperature of -50 ˚C, in order to remove excess of water. The femurs were pulverized using a mortar and pestle, without liquid nitrogen. The measurements of bone powder were performed with a 4 kW commercial wavelength dispersive X-ray fluorescence spectrometer (Bruker S4 Pioneer), using a Rh X-ray tube with a 75 mm Be end window and a 34 mm diameter collimator mask. Measurements were performed in helium mode and using high-density polyethylene X-ray fluorescence sample cups with 35.8 mm diameter assembled with a 4 mm prolene film to support the bone sample. The polyethylene cup was placed in steel sample cup holders with an opening diameter of 34 mm. The percentage of calcium and phosphorus was measured in the analysed samples.

Mechanical Tests

Mechanical tests allow us to determine the behaviour of bone under a load. Briefly, the Young's modulus is a measure the stiffness of a material, the strength or yield strength is defined as the stress at which a material begins to deform plastically, and the toughness is the ability of a material to absorb energy and plastically deform without fracturing[61] (Fig.1).

Compression tests of human bone

The 15 mm cylinders of human bone were defatted for 3 hours using a chloroform and methanol (1:1) solution and were hydrated overnight in PBS 1x prior to testing. The tops of the cylinder were cut and polished, so that the samples are composed only by trabecular bone. Compression tests were performed in a universal testing machine (Instron 5566™, Instron Corporation) with a 10-kN load cell and a cross-head rate of 0.1 mm/s. Stress–strain curves were obtained for each sample using the Bluehill 2 software (Instron Corporation). This software has the ability to build stress–strain representations from load displacement points, normalized for the dimensions of the specimen. The respective curves were analysed in order to obtain the mechanical bone

parameters: stiffness (Young's modulus), strength (yield stress), and toughness (energy absorbed until fracture)[62] - see Fig.3.

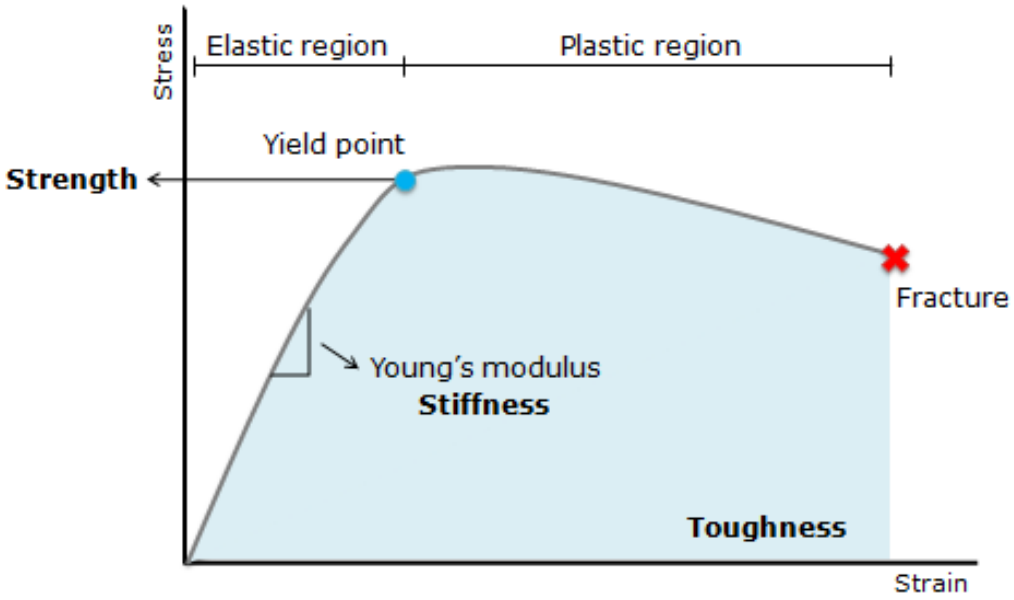

Figure 3 Graphical representation of the parameters evaluated from bone mechanical compression test. The yield point is the point where a material loses its elastic behaviour and occurs the first microfractures; Young's modulus or Stiffness is a measure of bone resistance to deformation; Toughness or energy until failure is the energy required to induce failure of the structure which corresponds to the Fracture of bone structure[62]

Three-point bending of rat femur

For the three-point bending test the femur was placed on two supporting pins a set 5mm apart and a third loading pin is lowered from above at a constant rate until sample failure. The bending load was applied to the femoral midshaft perpendicularly to the long axis of the bone until failure of the specimen[63]. Tests were performed using the same equipment and analysis software as in the mechanical compression tests, under the same conditions. The respective curves were analysed in order to obtain the mechanical bone parameters: yield stress and ultimate stress (Fig. 4). In figure 2, yield point corresponds to yield stress and ultimate point corresponds to ultimate stress.

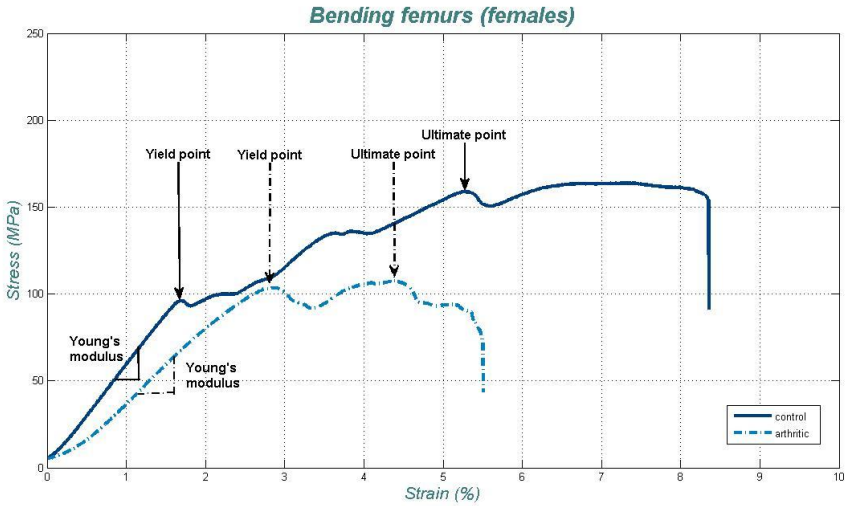

Figure 4 Graphical representation of the parameters evaluated by three point bending of femurs[63] . Yield point: the point where the bone tissue ceases to behave elastically; Ultimate point: is the maximum load that bone tissue can support while being stretched or pulled before failing or breaking (slope of the curve between the origin and the first yield point): is a measure of the stiffness of an elastic material like bone tissue; The trace line correspond to arthritic rats and the full line to healthy rats; Yield point corresponds to yield stress and ultimate point corresponds to ultimate stress

Gene expression studies

Gene expression allows us to understand the effect of inflammation in bone at the molecular level. In this study we performed quantitative real-time-polymerase chain reaction (qRT-PCR) in order to evaluate if selected genes are being more or less expressed when patients have RA or rats have arthritis.

RNA extraction

Without defrosting the sample, small trabecular pieces were pulverized using a mortar and pestle. Bone powder was placed in TRIzol reagent and homogenized. Lipid solubilisation was performed with chloroform and the supernatant containing the RNA was preserved. Proteinase K digestion was performed at 55ºC. For the precipitation of RNA we used ice-cold isopropyl alcohol and the pellet containing the RNA was preserved and washed with ethanol 75%. The remaining RNA pellet was dissolved in RNase/DNase-free water. RNA was cleaned using a commercial kit (RNeasy mini kit, Qiagen) according to the manufacturer instructions. Genomic DNA contaminants were removed with DNaseI treatment (Qiagen). For rat samples the RNA extraction was performed using the same protocol, but instead of bone pieces we used the left tibia.

RNA concentration was determined spectrophotometrically (Nanodrop ND-1000 Spectrophotometer, Thermo Fisher Scientific). RNA was stored at –80ºC and later used for complementary (c)DNA synthesis.

cDNA synthesis

cDNA synthesis was performed on 3ng of RNA from each sample using the DyNAmo cDNA synthesis kit (Thermo Fisher Scientific) and 300 ng of random hexamers according to the manufacterer's instructions. The reverse transcription reaction was performed on a thermocycler at 37ºC for 30 minutes for cDNA synthesis followed by a 85ºC for 5 minutes incubation to stop the enzyme activity. The cDNA template were stored at -20ºC for qRT-PCR.

Quantitative real time-polymerase chain reaction (qRT-PCR)

Each cDNA sample with a concentration of 3ng/µL was amplified in duplicate with DyNAmo Flash SYBR green qPCR kit (Thermo Fisher Scientific) in the RotorGene 6000 thermocyler (Qiagen) according to the manufacturer's instructions. The reaction starts at 50ºC for 2 minutes and then 95ºC for 7 minutes, followed by denaturation at 95ºC for 10 seconds and annealing at 60ºC for 10 seconds for 50 cycles. The reactions were validated by the presence of a single peak in the melt curve analysis.

The results were analysed by the standard curve method. The standard curves were made using cDNA templates with known RNA concentration from individuals with normal BMD and without clinical risk factors for osteoporosis. The cycle threshold (C_T) is defined as the number of cycles required for the fluorescent signal to cross the threshold and exceed the background level. The efficiency of the PCR should be between 90-100%, which means that for each cycle the amount of product doubles. The conversion of the C_T value in relative expression levels was performed applying the equation $10^{(CT - Y\ intersect\ /slope)}$ in which slope and Y intersect were extracted from standard curve[64,65]. Primers for the housekeeping and target genes were designed using the software Probefinder[66] in order to anneal in separate exons preventing amplification of contaminating DNA. The values obtained with qRT-PCR were normalized with the housekeeping gene phosphomannomutase 1 (PMM1) for human samples and Ribossomal protein 29 (RSP29) for rat samples. Primers sequence and details can be found in Annex 1.

Statistical analysis

Results are presented as mean and standard deviation for continuous variables and categorical variables are presented as relative frequencies.

In humans, the RA patient group of interest was compared with the primary OP control group and OA control group. OP control group allow us to compare the inflammatory interaction of disease and the OA control group, the loss of bone mineral density. The normality of continuous variables was tested with Shaphiro-Wilk test, and either Student's t test or the non-parametric Mann-Whitney test was used to compare RA with OP and RA with OA. In rats we used the same approach to compare the healthy with the arthritic group.

For categorical variables, chi-squared test was used. Significance level was set as 0.05. Statistical analysis was performed using the Statistical Package for Social Sciences manager software, version 17.0 (SPSS, Inc). All graphics were created using GraphPrad Prism sofware, version 5 (GraphPad Software, Inc).

Results

Human samples – RA vs OA

Patient characteristics

For this study 12 patients with RA were recruited. As controls age and sex matched 14 patients with OP, and 14 with OA were also recruited (Tables 1 and 4). RA patients have a mean age of 65±15 years, and this population was composed by 83% of women with disease duration of 4.74±3.29 years. The mean t-score for these patients was -2.72±0.78 and they had a mean BMD of 0.68±0.06 g/cm^2. These patients have a mean DAS28 3V of 4.19±2.13. All RA patients were under corticosteroid therapy, but only 72.7% of them were under methrotrexate, and only one was under biological therapy (Etanercept). Sixty percent of RA patients were positive to anti-cyclic Citrullinated Peptide (anti-CCP) and 56% were positive to rheumatoid factor (Table 1).

Table 1 Clinical and biochemical characteristics of RA and OA patients

	RA (n=12)	OA (n=14)	p value
Age (years)	65±15	68±6	0.938
Women (%)	83	71	0.468
BMI (Kg/m2)	25.99±4.73	28.33±4.56	0.226
T-score	-2.72±0.78	-	-
BMD (g/cm2)	0.68±0.06	-	-
DAS28 3V	4.19±2.13	-	-
Methotrexate (%)	72.7	-	-
Corticosteroids (%)	100	-	-
Anti-CCP + (%)	60	-	-
RF + (%)	55.6	-	-
Disease duration (years)	4.74±3.29	-	-

Values represent mean±standard deviation; RA - Rheumatoid arthritis; OA - Osteoarthritis: BMI - Body mass index; BMD – Bone mineral density; Anti-CCP - Anti-cyclic citrullinated Peptide; RF – Rheumatoid factor

The OA population has a mean age of 68±6 years, and is composed by 71% of women. None of OA patients were under corticosteroids therapy (Table 1).

Bone turnover markers

When comparing serum bone turnover markers between RA and OA patients, no statistically significant differences were found. The CTX-I/P1NP ratio which reflects the balance between bone resorption and bone formation, no differences were found (Fig.5).

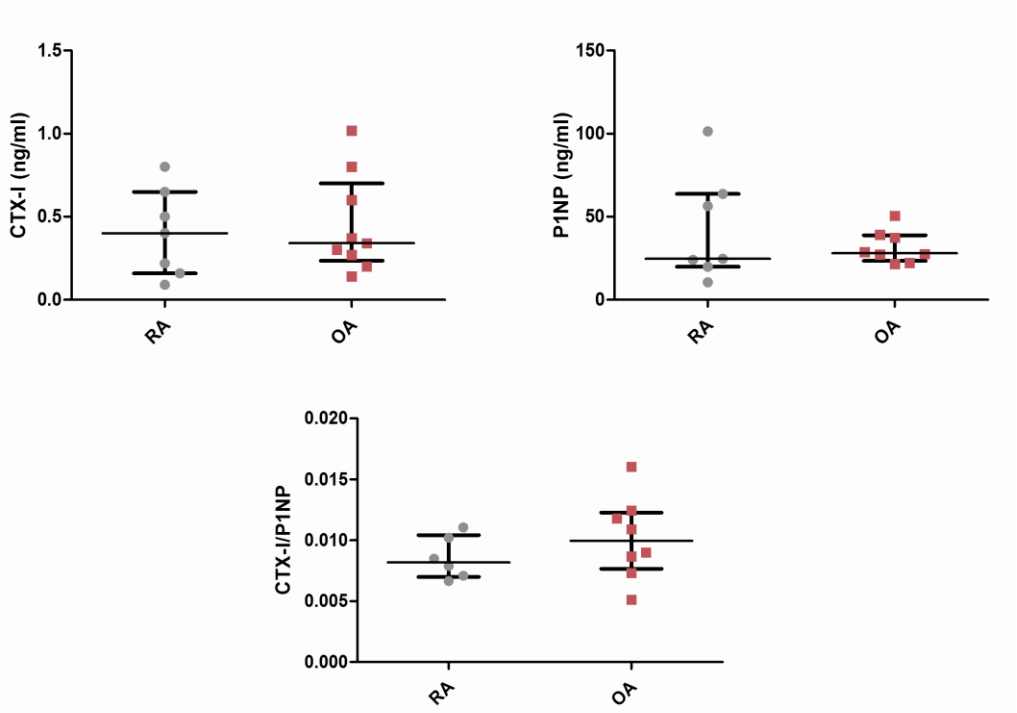

Figure 5 Levels of CTX-I, a marker of bone resorption, and P1NP, a marker of bone formation, and the calculated ratio of CTX-I/P1NP in RA and OA groups. Lines represent the median and interquartile range (10-90); RA - Rheumatoid arthritis; OA – Osteoarthritis; CTX-I - C-terminal cross-link telopeptide of type I collagen; P1NP - N-propeptide of type I collagen

Mechanical Compression Tests

To access bone mechanical characteristics, we performed compression tests and compared three parameters between RA and control groups: yield stress, Young's modulus and energy until failure.

No differences were found in any of these parameters when RA patients were compared with the OA patients (Table 2) but the young's modulus was slightly decreased in RA patients.

Table 2 Bone mechanical characteristics in RA and OA patients

	RA (n=12)	OA (n=14)	p value
Yield stress (MPa)	5.20 [2.21-9.02]	4.41 [2.48-10.70]	0.447
Young's modulus (MPa)	267.5 [88.33-544.0]	425.1 [224.90-690.0]	0.141
Energy until failure (MJ/m^3)	0.05 [0.02-0.12]	0.02 [0.01-0.19]	0.885

Values represent median [interquartile range 25-75]; RA - Rheumatoid arthritis; OA - Osteoarthritis: MPa - Mega Pascal; MJ - Mega Joule

Gene expression

In order to determine the effect of RA at the gene level, we performed gene expression of trabecular bone. None of the studied genes shows statistically significant differences, although we can see a tendency for most of osteoblasts markers (COL1A1, OPG, RANKL, OSX and LRP6) to be increased in RA patients when compared to OA patients. WNT10B, a protein of the Wnt family and is receptor SOST

have a higher expression in OA group than RA, however with no statistically significant difference (Table 3).

Table 3 Gene expression from trabecular bone of RA and OA patients

	RA (n=12)	OA (n=14)	p value
COL1A1	0.13 [0.04-0.24]	0.03 [0.01-0.09]	0.054
RUNX2	0.16 [0.01-0.23]	0.11 [0.05-0.17]	0.580
OSX	0.15 [0.002-0.29]	0.05 [0.02-0.36]	0.794
OPG	0.24 [0.02-0.73]	0.08 [0.01-0.16]	0.123
RANKL	0.53 [0.02-2.14]	0.08 [0.02-0.16]	0.158
RANKL/OPG	2.23 [0.28-5.72]	1.01 [0.32-4.32]	0.762
ALP	0.07 [0.01-0.34]	0.03 [0.02-0.05]	0.235
OCN	0.02 [0.004-0.32]	0.03 [0.007-0.09]	0.821
SEMA 3A	0.36 [0.16-1.79]	0.25 [0.06-0.29]	0.159
WNT10B	1.70 [0.17-2.07]	10.42 [0.03-40.91]	0.342
LRP5	0.08 [0.02-0.13]	0.07 [0.03-0.14]	0.944
LRP6	0.16 [0.01-0.31]	0.04 [0.03-0.09]	0.973
SFRP1	0.03 [0.003-0.14]	0.04 [0.01-0.19]	0.434
DKK1	0.01 [0.04-0.24]	0.01 [0.004-0.04]	0.762
DKK2	0.07 [0.01-0.17]	0.02 [0.01-0.07]	0.214
WIF1	2.29 [0.45-16.05]	2.42 [0.93-6.57]	0.768
SOST	0.03 [0.01-0.28]	0.20 [0.05-0.80]	0.157

Values represent median [interquartile range 25-75]; Gene expression is normalized to the housekeeping gene PMM1 (phosphommanomutase-1); RA - Rheumatoid arthritis; OA - Osteoarthritis: COL1A1 - Collagen, type I alpha 1; RUNX2 - Runt-related transcription factor 2; OPG – Osteoprotegerin; RANKL - receptor activator of nuclear factor kappa B ligand; OSX – Osterix ; ALP – Alkaline phosphatase; OCN – Osteocalcin; SOST – slcerostin; WNT10B - Wingless-type MMTV integration site family, member 10B; LRP - Low-density lipoprotein receptor-related protein; SFRP1 - Secreted frizzled-related protein 1; DKK - Dickkopf-related protein; WIF1 - Wnt inhibitory factor 1; SEMA 3A - Semaphorin-3A

Human samples – RA vs OP

Osteoporosis population

The RA population is already described above. The OP patients have a mean age of 73±6 years, with 86% of women. These patients have a mean T-score of -2.67±0.60 and mean BMD of 0.67±0.09 g/cm^2. Both RA and OP patients have similar BMD and T-score (Table 4).

Table 4 Clinical and biochemical characteristics of RA and OP patients

	RA (n=12)	OP (n=14)	p value
Age (years)	65±15	73±6	0.163
Women (%)	83	86	0.867
BMI (Kg/m2)	25.99±4.73	23.73±2.82	0.182
T-score	-2.72±0.78	-2.67±0.60	0.926
BMD (g/cm2)	0.68±0.06	0.67±0.09	0.757
DAS28 3V	4.19±2.13	-	-
Methotrexate (%)	72.7	-	-
Corticosteroids (%)	100	0	-
Anti-CCP + (%)	60	-	-
RF + (%)	55.6	-	-
Disease duration (years)	4.74±3.29	-	-

Values represent mean±standard deviation; RA - Rheumatoid arthritis; OA - Osteoarthritis; BMI - Body mass index; BMD – Bone mineral density; Anti-CCP - Anti-cyclic citrullinated Peptide; RA factor – Rheumatoid factor

Bone turnover markers

On the comparison of RA with OP patients we found a decrease in P1NP level in RA patients, although without reaching statistical significance. No differences were found on bone turnover ratio CTX-I/P1NP (Fig.6).

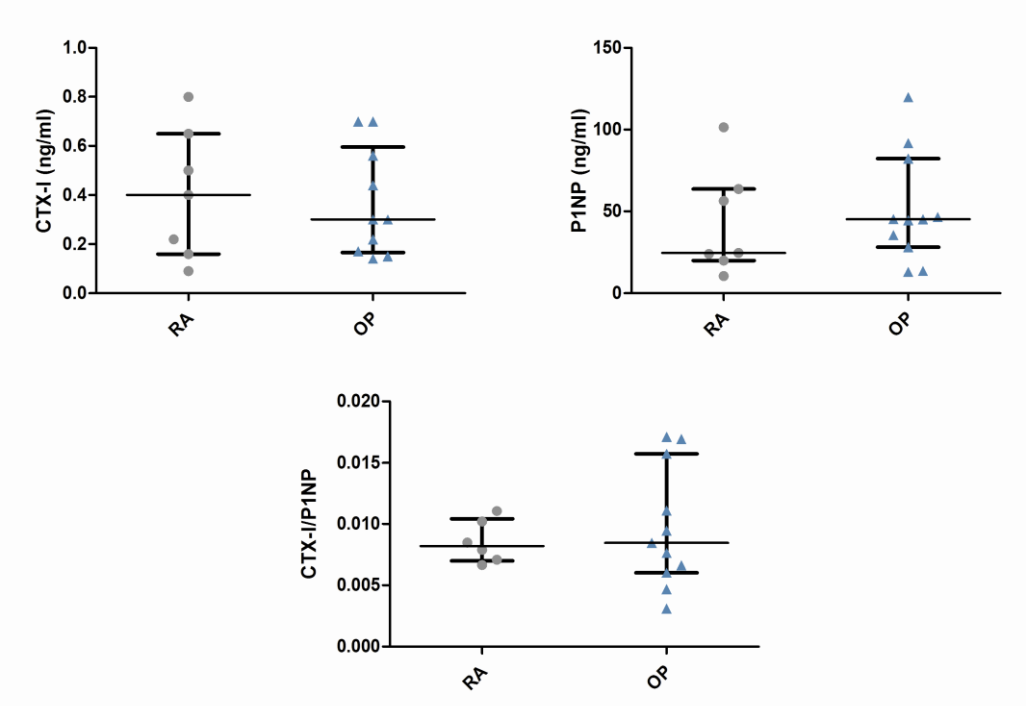

Figure 6 Comparison between RA group and OP group of the serum bone markers quantification and bone turnover ratio; Lines represent the median and interquartile range (10-90); RA - Rheumatoid arthritis; OA – Osteoarthritis; CTX-I - C-terminal cross-link telopeptide of type I collagen; P1NP - N-propeptide of type I collagen

Mechanical Compression Tests

When we compare the yield stress, Young's modulus and energy until failure of RA and OP patients, no significant differences were found when comparing bone mechanical properties (Table 5).

Table 5 Bone mechanical characteristics in RA and OP patients

	RA (n=12)	OP (n=14)	p value
Yield stress (MPa)	5.20 [2.21-9.02]	3.61 [2.08-8.59]	0.598
Young's modulus (MPa)	267.5 [88.33-544.0]	221.8 [140.20-329.4]	0.374
Energy until failure (MJ/m^3)	0.05 [0.02-0.12]	0.07 [0.03-0.16]	0.440

Values represent median [interquartile range 25-75]; RA - Rheumatoid arthritis; OA - Osteoarthritis: MPa - Mega Pascal; MJ - Mega Joule

Gene expression

Gene expression of trabecular bone of OP patients was also performed and compared with the RA patients.

We found that both COL1A1 (p=0.009) and RANKL (p=0.007) were significantly decreased in RA patients when compared with the OP group (Table 6 and Figure 7). Moreover we also found that, WNT10B (p=0.004), SFRP1 (p=0.016) and DKK1 (p=0.005) are decreased in RA when compared to OP patients. No other significant differences were found, however there is a tendency for RA osteoblast gene expression to be decreased when compared to OP patients (Table 6).

Table 6 Gene expression from trabecular bone of RA and OP patients

	RA (n=12)	OP (n=14)	p value
COL1A1	0.13 [0.04-0.24]	0.91[0.02-2.39]	0.009 **
RUNX2	0.16 [0.01-0.23]	0.21[0.13-0.40]	0.136
OSX	0.15 [0.002-0.29]	0.16 [0.07-52.31]	0.140
OPG	0.24 [0.02-0.73]	0.55 [0.19-2.23]	0.176
RANKL	0.53 [0.02-2.14]	5.25 [0.62-35.20]	0.007 **
RANKL/OPG	2.23 [0.28-5.72]	3.87 [3.01-6.46]	0.121
ALP	0.07 [0.01-0.34]	0.21 [0.08-0.73]	0.100
OCN	0.02 [0.004-0.32]	0.01 [0.003-0.02]	0.160
SEMA 3A	0.36 [0.16-1.79]	0.57 [0.40-1.75]	0.439
WNT10B	1.70 [0.17-2.07]	9.27 [2.75-11.29]	0.004 **
LRP5	0.08 [0.02-0.13]	0.51 [0.04-1.52]	0.132
LRP6	0.16 [0.01-0.31]	0.80 [0.06-1.51]	0.140
SFRP1	0.03 [0.003-0.14]	10.46 [0.05-22.91]	0.016 *
DKK1	0.01 [0.04-0.24]	3.06 [1.41-31.13]	0.005 **
DKK2	0.07 [0.01-0.17]	0.30 [0.06-16.46]	0.110
WIF1	2.29 [0.45-16.05]	5.44 [1.99-8.51]	0.695
SOST	0.03 [0.01-0.28]	0.22 [0.06-145.80]	0.087

Values represent median [interquartile range 25-75]; Gene expression is normalized to the housekeeping gene PMM1 (phosphommanomutase-1); **p<0.01; RA - Rheumatoid arthritis; OP - Osteoporosis; COL1A1 - Collagen, type I alpha 1; RUNX2 - Runt-related transcription factor 2; OPG - Osteoprotegerin; RANKL - receptor activator of nuclear factor kappa B ligand; OSX - Osterix ; ALP - Alkaline phosphatase; OCN - Osteocalcin; SOST - Slcerostin; WNT10B - Wingless-type MMTV integration site family, member 10B; LRP - Low-density lipoprotein receptor-related protein; SFRP1 - Secreted frizzled-related protein 1; DKK - Dickkopf-related protein; WIF1 - Wnt inhibitory factor 1; SEMA 3A - Semaphorin-3A

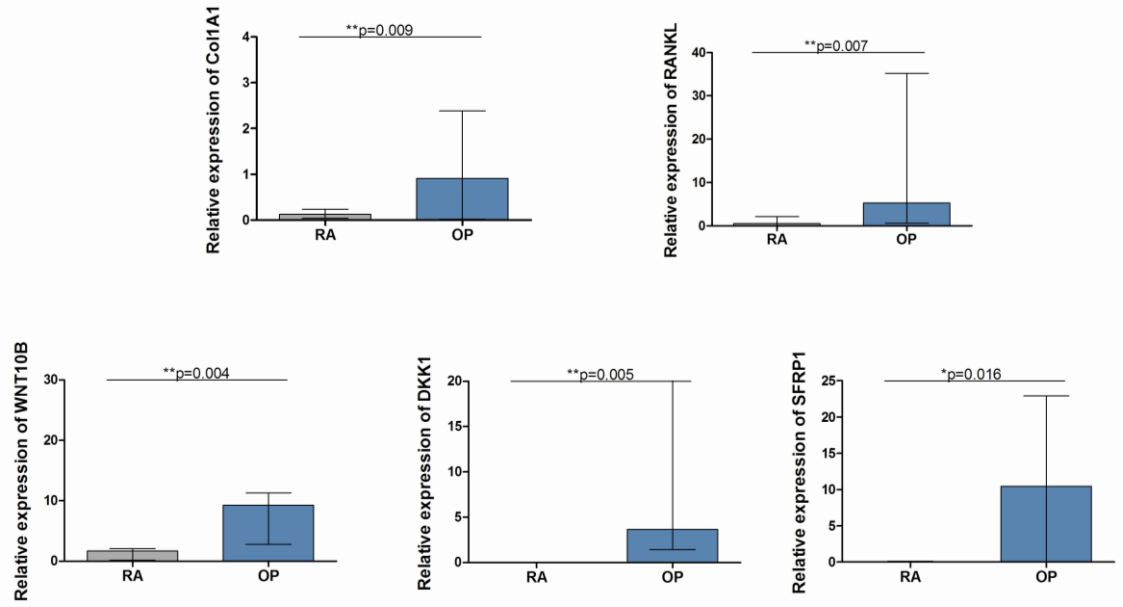

Figure 7 Osteoblast markers and Wnt-related genes with statistical difference between RA e OP patients. Bars represent median [interquartile range 25-75]; Gene expression was normalized to the housekeeping gene PMM1 (phosphommanomutase-1); *p<0.05, **p<0.01; RA - Rheumatoid arthritis; OA – Osteoarthritis; OP - Osteoporosis; COL1A1 - Collagen, type I alpha 1; RANKL - receptor activator of nuclear factor kappa B ligand; WNT10B - Wingless-type MMTV integration site family, member 10B; DKK - Dickkopf-related protein; SFRP1 - Secreted frizzled-related protein 1

As mentioned by Caetano-Lopes and co-workers[67], gene expression in bone fluctuates during fracture healing. For this reason we divided the fragility fracture patients (OP group) in three sub groups depending on the days between fracture and surgery: the first, until 3 days post-fracture, the second, between 4 and 7 days post-fracture and the third with 8 or more days post-fracture. We found no significant differences throughout time in any of the analyzed genes (Fig.8).

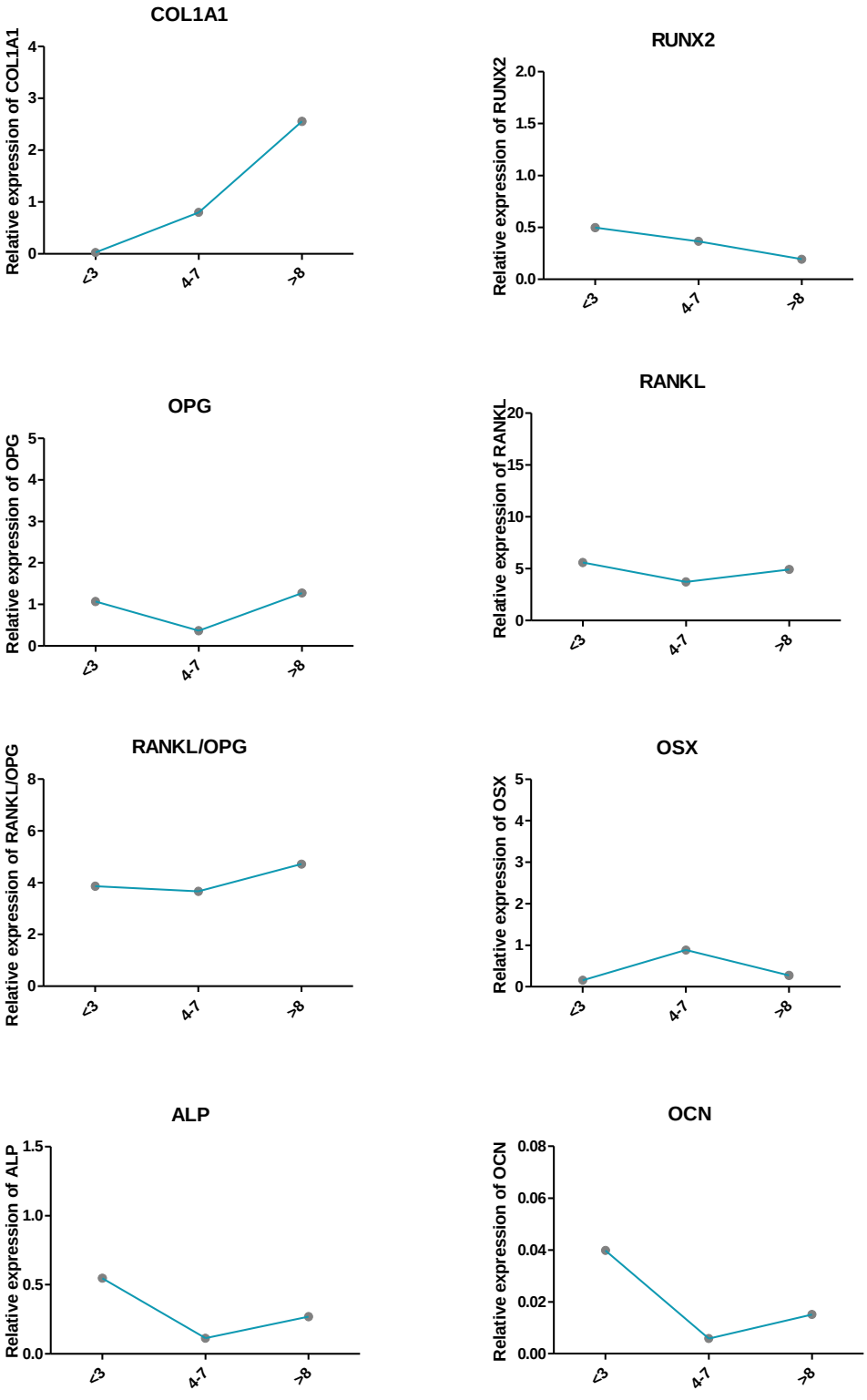

Figure 8 Relative gene expression of osteoblast markers according to the time between fracture and surgery; Dots represent median values; gene expression was normalized to PMM1. COL1A1 - Collagen, typ e I, alpha 1; Runx2 - Runt-related transcription factor 2; OPG – Osteoprotegerin; RANKL - receptor activator of nuclear factor kappa B ligand; OSX – Osterix ; ALP – Alkaline phosphatase; OCN – Osteocalcin; PMM1 - phosphomannomutase 1

Immunohistochemistry of femoral epiphysis

Immunohistochemistry analysis could not be performed due to technical reasons. Femoral epiphyses were stored at -80ºC before sample processing. Due to this low temperature, most of the epitopes were destroyed. For this reason we could not confirm our gene expression results. In Fig.9 representative images of immuhistochemistry in selected samples of RA without epitope destruction are shown.

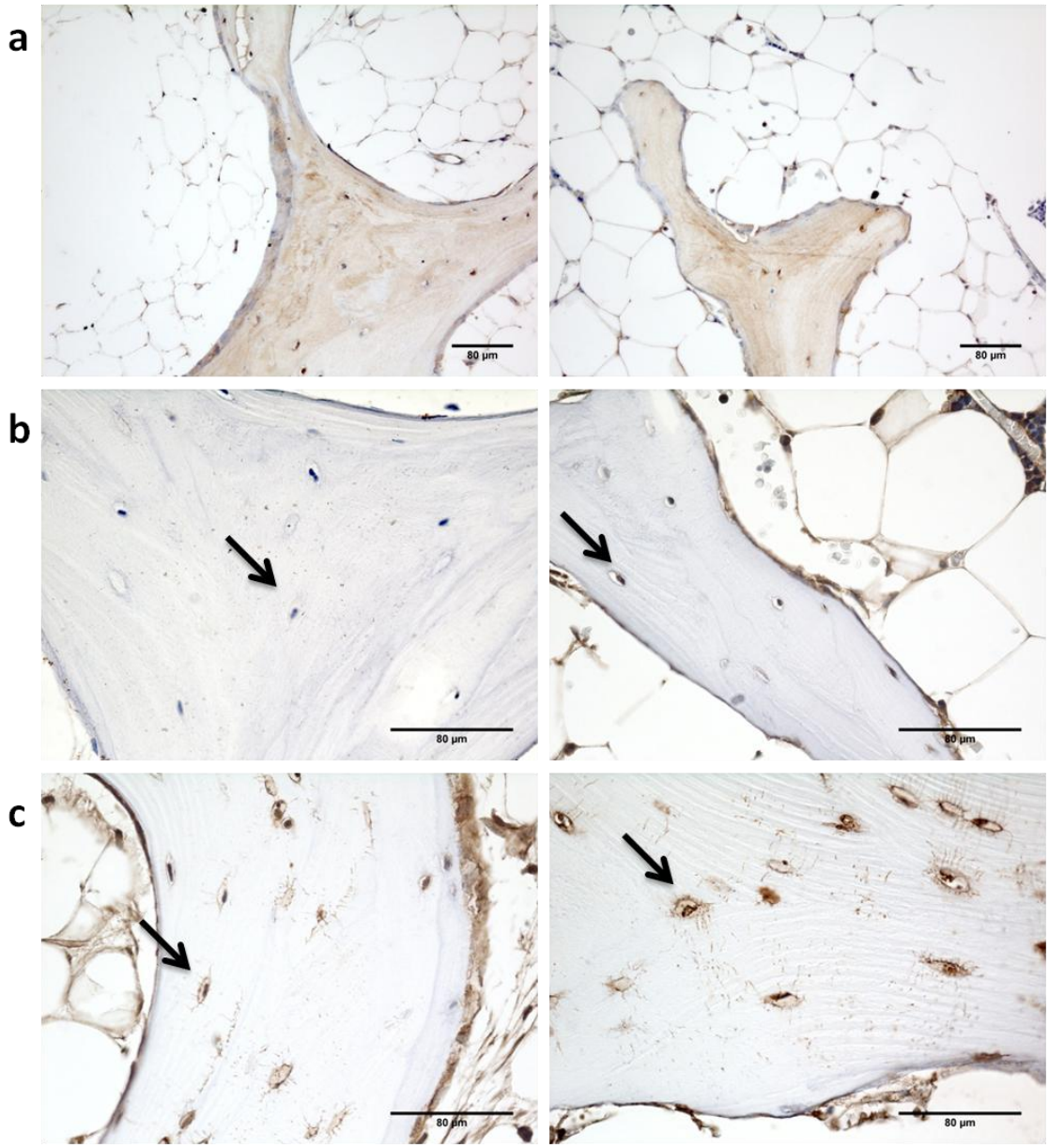

Figure 9 Immunohistochemistry of two RA samples, the pictures on the left are from a 26 years-old female and on the right of a 77 years-old men; a) Anti-OCL which stains osteoblast and mineralized bone in brown were osteocalcin is embedded, 20x objective; b) Anti-DKK1 stains osteocytes where DKK1 is produced, the black arrow shows osteocytes, 40x objective; c) Anti-SOST stains osteocytes where sclerostin is produced, black arrow shows osteocytes. 40x objective.

Rat model of arthritis

Nine AIA rats were used and as controls 12 healthy Wistar rats were used.

The inflammatory score, ankle perimeter and body weight were measured during the study period every other day. At the time of sacrifice vertebrae and long bones, such as femur and tibia, were collected for histological evaluation, RNA extraction and three point bending test. Blood samples were collected by cardiac puncture for bone turnover markers assessment.

Clinical assessment

Throughout disease duration, the inflammatory score, weight and ankle perimeter were access in order to observe the physical effect of arthritis. The inflammatory score is significantly increased in the arthritic rats when compared to the healthy ones ($p<0.001$, Fig.10) and reaches a plateau at days 19-20 of disease. Before day 10 post induction there were no differences in weight between the two groups (Fig 10). However, after day 10, the weight of the arthritic group starts to decrease with statistically significantly differences after 14th day of disease. The ankle perimeter of the healthy group has a mean of 2 centimetres during the 22 days of the study, while in the arthritic group the perimeter increases significantly after the 12th day post disease induction (Fig.10).

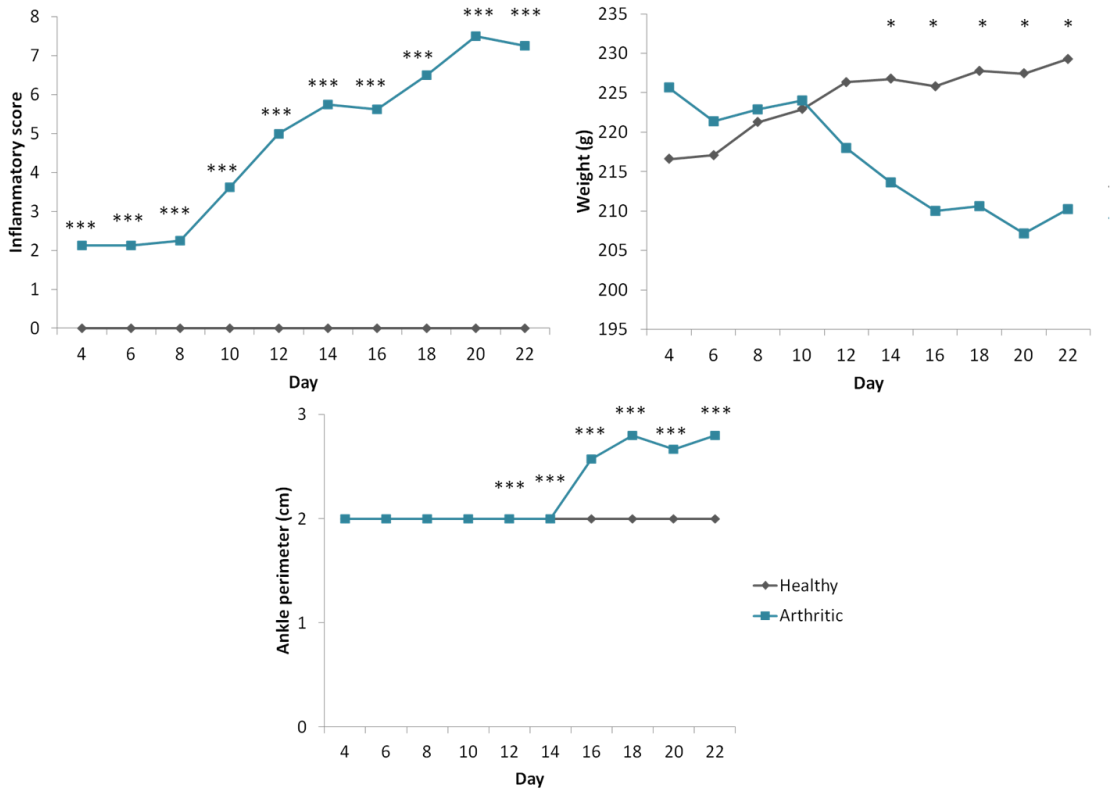

Figure 10 Inflammatory score, weigh and ankle perimeter oh healthy and arthritic rats during the 22 days of experiment. Inflammatory score of healthy and arthritic rats during the 22 days of the experiment showing a marked increase at day 8 and a plateau at days 19-20. Weight of arthritic rats decreases after day 10. Ankle perimeter of arthritic rats increases after day 12. Each point represents the mean of the group for each day; *p<0.05;***p<0.001

Bone turnover markers

To access bone turnover, serum levels of CTX-I and P1NP were determined. The bone resorption marker CTX-I was significantly higher on the arthritic group (p=0.003) but no differences were found in P1NP levels, although it was increased in the arthritic rats (Fig.11). CTX-I/P1NP ratio was not significant different between the healthy and arthritic rats.

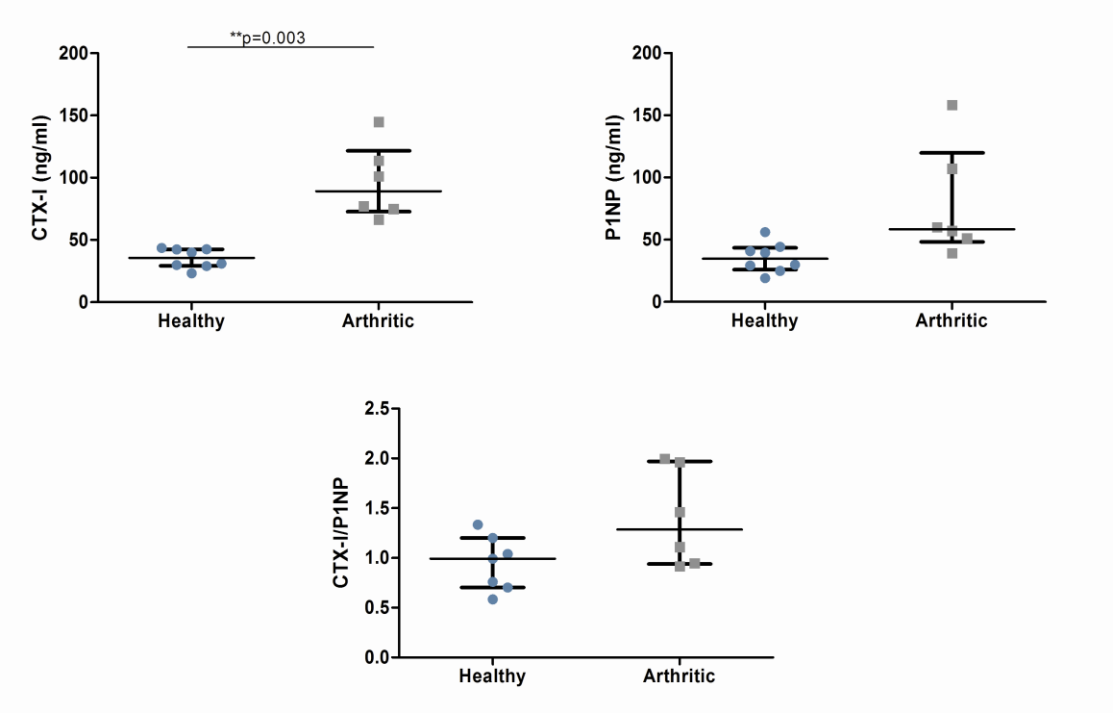

Figure 11 CTX-I and P1NP serum concentrations measured in rat serum 22 days after arthritis induction and the CTX-I/P1NP ratio. Lines represent median and interquartile range (10-90); **p<0.01; CTX-I - C-terminal cross-link telopeptide of type I collagen; P1NP - N-propeptide of type I collagen

Histomorphometry

In order to look at the bone microstructure and organization, parameters were evaluated by histomorphometry of the 4th lumbar vertebra at day 22 post-disease induction. Bone volume (BV/TV) was significantly decreased in the arthritic rats (p<0.0001) while trabecular separation (Tb.Sp) is significantly increased (p=0.009; Fig.12). Trabecular thickness (Tb.Th) although it is slightly decreased in arthritic rats, showed no difference between the groups.

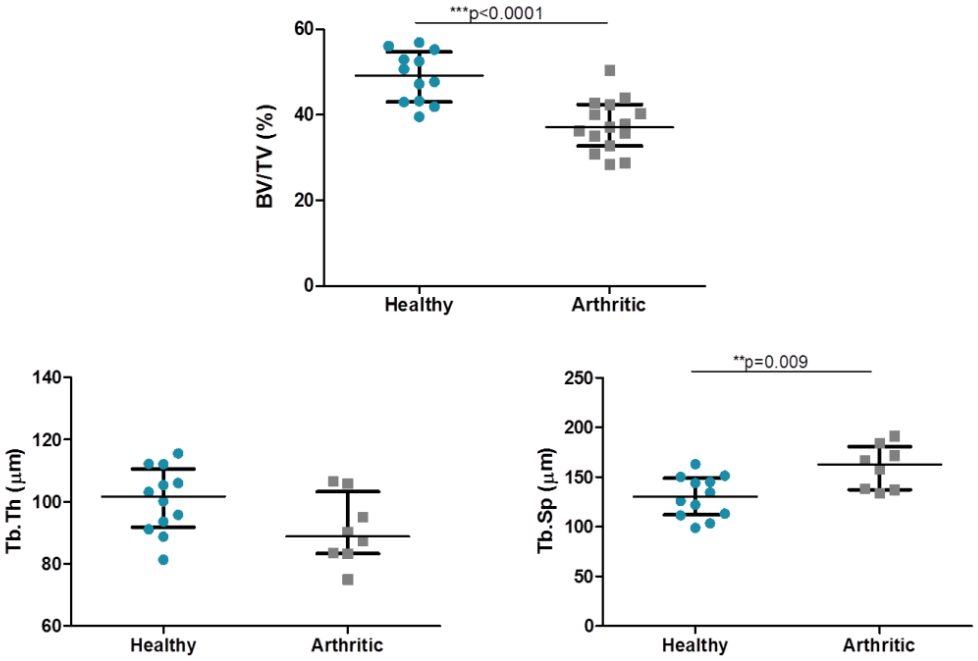

Figure 12 Comparison of BV/TV, Tb.Th and Tb.Sp between healthy and arthritic groups 22 days after disease induction; **p<0.01; ***p<0.001. Lines represent median and interquartile range (10-90). BV/TV – Bone volume; Tb.Th - Trabecular thickness; Tb.Sp - Trabecular separation

Energy-dispersive X-ray spectroscopy

Hydroxyapatite ($Ca_5(PO_4)_3(OH)$) crystals are formed by calcium and phosphorus, so it is important to quantify their proportion on bone. Both calcium and phosphorous are significantly reduced in arthritic rats (p=0.041 and p=0.031, respectively; Fig.13 compared to the control group).

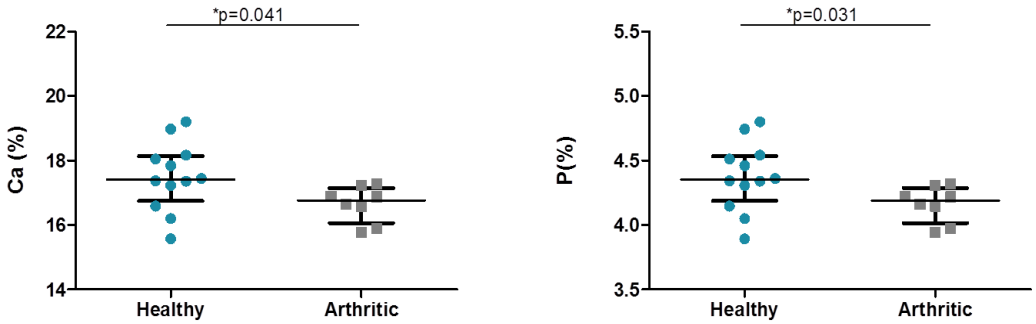

Figure 13 Calcium (Ca) and Phosphorus (P) proportion on bone of healthy and arthritic groups 22 days after disease induction; Lines represent median and interquartile range (10-90); *p<0.05

Three-point bending

In order to determine the mechanical bone behaviour under a loading force a three-point bending test was performed. Yield stress is a measure of elasticity and the ultimate stress is the energy at which the first microfracture occurs. Both yield stress

and ultimate stress, were significantly decreased in arthritic femurs (p=0.005 and p=0.026 respectively; Fig.14).

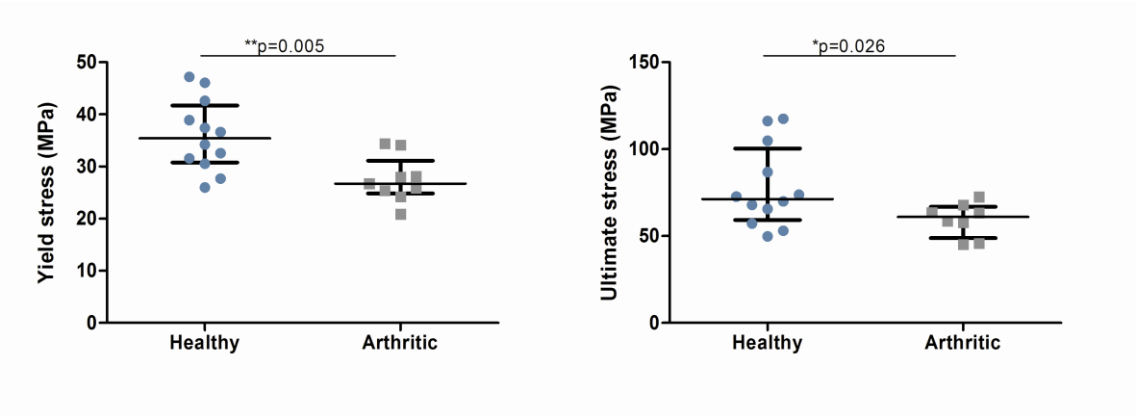

Figure 14 Bone mechanical properties (yield stress and ultimate stress) were assessed in healthy and arthritic groups; Lines represent median and interquartile range (10-90) *p<0.05, **p<0.01

Gene expression

For the animal model of arthritis we studied osteoblast and osteoclast specific genes, as well as some involved in the Wnt signalling pathway in bone samples from both groups. When comparing healthy and arthritic rats we found that OPG levels are decreased in the arthritic animals as is RANKL, CTSK and LRP6 expression. However, no significant differences in any of the studied genes were found (Table 7).

Table 7 Gene expression in bone from healthy and arthritic rats

OCN	60.01 [31.31-147.3]	78.18 [51.23-102.0]	0.80
RANKL	1.18 [0.47-11.56]	0.86 [0.31-3.12]	0.448
OPG	75854 [35765-136176]	59556 [29432-77259]	0.279
RANKL/OPG	$1.29x10^{-5}$ [$0.53x10^{-5}$-$4.82x10^{-5}$]	$1.23x10^{-5}$ [$0.34x10^{-5}$-$8.49x10^{-5}$]	0.814
CTSK	269.2 [115.8-382.6]	92.51 [25.49-329.1]	0.105
WNT10B	2.12 [1.51-4.35]	2.21 [0.62-8.51]	0.654
LRP6	1.29 [0.87-1.76]	0.46 [0.27-1.29]	0.052
WIF1	0.91 [0.60-1.16]	0.77 [0.24-1.54]	0.954

Values represent median [interquartile range 25-75]; OCN – Osteocalcin; OPG – Osteoprotegerin; RANKL - receptor activator of nuclear factor kappa B ligand; CTSK – Cathepsin K; LRP6 - density lipoprotein receptor-related protein 6; WNT10B - WNT10B Wingless-type MMTV integration site family, member 10B; WIF1 - Wnt inhibitory factor 1

Discussion

The aim of this study was to analyse the effect of rheumatoid arthritis in the bone quality and microstructure level and also osteoblast and Wnt-related gene expression.

For this work, we recruit RA patients with active disease (DAS18 3V Hospital de Santa Maria). RA patients had a mean age of 65 years with mean disease duration of 4.74 years. Our RA population was composed mostly by women (83%), which is in accordance with Alamanos' epidemiology study of RA prevalence in the female gender. Sixty percent of RA patients were positive for anti-CCP, a specific and early marker of RA and around 55% were positive for rheumatoid factor[68,69]. Around 70% of RA patients were under methotrexate, a commonly used disease-modifying anti-rheumatic drug (DMARD)[70] and all RA patients were under corticosteroid therapy. As controls, two groups were used, patients with osteoporosis and patients with osteoarthritis.

To complement the study of the influence of inflammation on Wnt pathway on bone, we used Wistar rats with adjuvant-induced arthritis as a model of arthritis and we studied bone microstructure, bone turnover ratio, mechanical properties and gene expression.

Humans – RA and AO patients

There were no differences between RA and OA patients in sex and age, but unlike RA patients, OA patients were not under corticosteroids.

We first wanted to adress bone quality parameters differences between RA and OA patients. Our results show no difference in serum bone turnover markers between RA and OA patients which is in accordance with Wislowska *et al.* who found no differences on serum concentrations of formation and resorption markers between RA and OA patients[71].

When comparing RA and OA patients' bone mechanical properties we found a slight decrease in Young's modulus but no statistical differences were found. Brown *et al*. showed that although there were biomechanical differences between the superior and inferior region of a femoral head in compressive modulus and yield strength, when they compared an OA femoral head with femoral heads with no features of OA, no differences were found[72]. Rodrigues *et al*. found that when patients with fragility fractures were compared with patients with osteoarthritis, the first have lower Young's modulus, yield stress and energy until failure[73]. Then in 2012, Rodrigues and co-workers showed that stiffness (Young's modulus) was significantly lower in patients with hip fractures comparing with osteoarthritis patients, suggesting that OA patients have better mechanical properties than patients with low BMD and fragility fractures although in our results we didn’t detected differences between the two groups.

At gene expression level, there was a tendency for increased expression of COL1A1, OPG, RANKL, OSX and LRP6 genes, and decreased expression of SOST and WNT10B in RA patients when compared with OA patients. However, none of these results were statistically significant. To the best of our knowledge there are no previous works comparing trabecular gene bone expression of SEMA 3A, WNT10B, LRP5/6, SFRP1, DKK1/2 or WIF1 between RA and OA patients. RANKL and OPG are pivotal molecules in the regulation of bone turnover. Xu *et al*. showed that serum RANKL, serum OPG and the calculated ratio were higher in RA than in healthy controls, which is in accordance with the role of RANKL/OPG on bone erosions and joint destruction[74].

Kotake and co-workers found that serum RANKL and the ratio RANKL/OPG were significantly higher in RA patients, while serum OPG was lower when compared to OA samples[75]. In our work, we found that both RANKL and OPG expression was higher in RA patients, although they did not reach statistical difference.

OSX and WNT10B are transcription factors essential for osteoblast differentiation from mesenchymal stem cells. In this work, we found that OSX and WNT10B expression was increased in RA patients when compared to OA samples, although these results did not reach statistical significance. In accordance, it was previously shown that OSX expression is higher in cultured adipose-derived mesenchymal stem cells (ASCs) from RA than OA patients[76]. Imai et al (2006) showed that WNT10B was highly expressed in lining cells and fibroblasts of RA patients when compared with OA and these results were confirmed by immunohistochemistry[77].

SFRP1 and SOST are inhibitors of the canonical wnt pathway and, therefore, inhibitors of osteoblast differentiation and, consequently, of bone formation. In accordance with our results, Ijiri et al (2002) did not found differences in SFRP1 gene expression between RA and OA fibroblast-like cells[78]. We also found a slight increase in SOST expression in RA patients when compared to OA samples. By immunohistochemistry, Appel *et al*. found that sclerostin expression by osteocytes on joints was slightly higher in RA patients when compared with ankylosis spondylitis, OA patients and controls. Comparing directly OA with RA patients, they found that the last group had higher expression of sclerostin[79].

One of the limitations of this study is the sample size, which might not be enough to detect differences between the two groups. Moreover, we were unable to access OA patients BMD which might be of help when interpreting the data and we lack a true control group without inflammation or any metabolic bone disease.

Overall, when comparing RA with OA bone we observed no differences in bone mechanics, serum turnover markers or bone gene expression.

Humans – RA and OP patients

Both our RA and OP cohorts of patients have osteoporotic T-scores (lower than -2.5) and low BMD (less than 0.7 g/cm^2)[80]. Accordingly, we found no differences on either serum P1NP or CTX-I levels, neither on the ratio CTX-I/P1NP when comparing RA and OP patients. These results are in accordance with previous studies that didn't found statistical differences between serum levels of these biomarkers between RA and OP patients[51]. Moreover, Xu *et al*. showed that both serum markers levels CTX-I and P1NP were higher in osteoporotic group when compared with the healthy controls[81]. Since RA and OP are characterized by loss of bone mass loss, we expected both groups to have similar levels of bone turnover markers. We also found no differences in bone biomechanical properties (Yield stress, Young's modulus and energy until failure), which is in accordance with previous studies who also didn't found any differences in any of these parameters[81].

When comparing gene expression, our results show a significant decrease on the expression of osteoblast genes COL1A1, RANKL and also on some Wnt signalling pathway genes as WNT10B, SFRP1 and DKK1 in RA patients when compared with OP patients. In accordance with our results, Patsch *et al*. showed that RANKL gene expression was higher in the group of men with idiopathic osteoporosis when compared with healthy controls[82]. Moreover it was shown that the RANKL/OPG ratio is

significantly higher in the bone marrow of patients with fractures as opposed to OA patients, but they did not find differences when compared gene expression in bone samples from the same groups[83]. Previous studies also showed that although serum RANKL was significantly decreased in RA when compared with OP patients no difference was found at the gene expression level[51]. Regarding the Wnt pathway players, Patsch and co-workers found that WNT10B expression was significantly higher in the group with idiopathic osteoporosis when compared with the healthy controls[82]. Moreover, it was described by Dovjak *et al* that DKK1 serum levels were increased in patients with hip fractures when compared with young controls[84]. D'Amelio *et al* shows that the expression of DKK1 was higher in the fractured patients, both in bone and bone marrow when compared to OA samples[83]. In contrast with our results, a previous study has shown no differences on serum DKK1 levels, but DKK1 gene expression was significantly higher in RA patients when compared to OP bone samples[51]. No studies describing SEMA3A, WNT10B, LRP5/6, SFRP1, DKK1/2 or WIF1 gene expression in human trabecular bone were found.

OP patients underwent hip replacement surgery due to fragility fracture, which might influence the expression of some of the genes studied. Therefore, we evaluated the expression of the same genes we compared between RA and OP patients in the post-fracture period. Comparing OP patients with different time between fracture and surgery, we found no differences in osteoblast's gene expression, which is in according with a previous study[67].

Again, this work has some limitations, namely the small sample size and the lack a true control group. Moreover, we studied gene expression at the bone microenvironment level including bone, bone marrow, fat and vessels making the results hard to interpret since some of the genes studied are not only expressed by osteoblasts but also by other cells in the surrounding environment.

Taken together, our results suggest that OP and RA patients have similar bone fragility but while OP is characterized by increased bone resorption[85], we show here that in RA bone the wnt pathway is downregulated, which might negatively influence bone formation and contribute to bone fragility.

Animal model

As expected, during the 22 post-induction days the inflammatory score of arthritic rats increases and they lose weight suggesting that the disease has a systemic effect. These symptoms are confirmed by Cai *et al.* (2006) who compared the effect of adjuvant-induced arthritis on Sprague-Dawley and Lewis rats[86].

When studying bone turnover, we found a high level of the bone resorption marker CTX-I in arthritic rats and a tendency to increase the bone formation marker P1NP. In accordance with our results, previous studies have described that in AIA model there is increased bone resorption by osteoclasts[15,14]. Moreover, Shopf and Noguchi, in different studies, described that collagen oligomeric matrix protein and CTX-I have higher levels in AIA arthritis when compared to the control group[15,87]. Using histomorphometry, we observed that arthritic rats have less bone volume with higher separation between trabeculae and a tendency for thinner trabeculae, which is in accordance with what has been described by Nanjundaiah *et al.*[88]. In accordance with our results, Osterman *et al.* performed histomorphometry in femoral metaphysic and found lower percent total bone area, trabecular thickness and trabecular number in the arthritic group when compared with healthy one, while trabecular separation was

significantly higher[89]. Noguchi *et al.* performed microCT of trabecular bone in calcaneous and found that BV/TV was significantly decreased in arthritic rats comparing to healthy ones[87].

To the best of our knowledge, there are no publications measuring arthritic rat bone mineral content with energy dispersive X-ray spectroscopy. When we compared the mineral content of healthy and arthritic bone, our results shown that arthritic rats have less calcium and phosphorus than healthy bones, which might indicate that there is no sufficient mineral for this bone to have a normal behaviour on mechanical tests. This different can be attributed to low calcium and phosphorus serum content or to poor osteoblast activity. Moreover, in accordance with these observations we found that the yield stress and ultimate stress of arthritic rats is significant lower than in healthy animals. Other studies in a mouse model of arthritis found that arthritic bone has significant worse mechanical properties with three-point bending test of femurs[63].

Regarding gene expression, no differences were found between arthritic and healthy rat samples. Several studies assessed the expression of bone-related genes on rat bone with contradictory results. Kishimoto *et al* found that in a collagen-induced arthritis model, that CTSK and RANKL expression was higher in arthritic when compared with the healthy rats, while OPG expression was decreased[90]. Ho *et al.* found that arthritic rats have higher levels of circulating RANKL, while OPG levels were similar between arthritic with healthy rats, and at gene expression level, both RANKL and OPG were higher in arthritic rats, as well as the ratio RANKL/OPG[91]. Engdahl *et al.* showed that RANKL expression was reduced in arthritic mice in synovial tissue, bone marrow and trabecular bone and OPG expression was significantly reduced in synovial, but not on bone marrow and trabecular bone when compared to healthy controls[92]. To the best of our knowledge no studies evaluated bone gene expression of OCL, WNT10B, LRP6 or WIF1.

The AIA model used in this work is a widely used model to study not only the physiopathology of arthritis but also to test the effect of drugs on the development of the disease. However, this model has an acute, rather than chronic, inflammation that resolves spontaneously over time. Although we believe that the effect of this resolution of inflammation might not be observed immediately on bone quality parameters, it may explain the lack of differences on gene expression between groups. Moreover, gene expression was performed in the bone microenvironment, rather than on bone and bone marrow separately, as was published by several works.

In summary, arthritic rats showed higher bone resorption, lower bone volume and trabecular separation and less mineral content, leading to worst mechanical properties. No differences were found at the gene expression level, which we believe to be a limitation of the model.

As conclusion, this thesis shows that RA bone fragility might be driven by osteoblast function deterioration, rather than by excessive bone resorption, through downregulation of the canonical Wnt pathway. More studies are needed to identify the mechanisms by which RA downregulates the Wnt canonical pathway.

References

1. Walsh, N. C. & Gravallese, E. M. Bone remodeling in rheumatic disease: a question of balance. *Immunol. Rev.* **233,** 301–312 (2010).

2. Gibofsky, A. Overview of epidemiology, pathophysiology, and diagnosis of rheumatoid arthritis. *Am. J. Manag. Care* **18,** S295–302 (2012).

3. Leibbrandt, A. & Penninger, J. M. RANK(L) as a key target for controlling bone loss. *Adv. Exp. Med. Biol.* **647,** 130–145 (2009).

4. Arboleya, L. & Castañeda, S. Osteoimmunology: The Study of the Relationship Between the Immune System and Bone Tissue. *Reumatol. Clínica* **9,** 303–315 (2014).

5. Walsh, N. C. *et al.* Osteoblast function is compromised at sites of focal bone erosion in Inflammatory Arthritis. *J. Bone Miner. Res.* **24,** 1572–1585 (2009).

6. Narducci, P., Bareggi, R. & Nicolin, V. Receptor Activator for Nuclear Factor kappa B Ligand (RANKL) as an osteoimmune key regulator in bone physiology and pathology. *Acta Histochem.* **113,** 73–81 (2011).

7. R. Orstavik, G. Haugeberg, P. Mowinckel, A. Hoiseth, T. Uhlig, J. Falch, J. Halse, E. McCloskey, T. K. Vertebral Deformities in Rheumatoid Arthritis. *Arch. Intern. Med.* **164,** 420–425 (2004).

8. Kim, S. Y. *et al.* Risk of osteoporotic fracture in a large population-based cohort of patients with rheumatoid arthritis. *Arthritis Res. Ther.* **12,** R154 (2010).

9. Takayanagi, H. Immunology and bone. *J. Biochem.* **154,** 29–39 (2013).

10. Guerrini, M. M. & Takayanagi, H. The immune system, bone and RANKL. *Arch. Biochem. Biophys.* (2014). doi:10.1016/j.abb.2014.06.003

11. Lubberts, E. *et al.* Increase in expression of receptor activator of nuclear factor kappaB at sites of bone erosion correlates with progression of inflammation in evolving collagen-induced arthritis. *Arthritis Rheum.* **46,** 3055–3064 (2002).

12. Crotti, T. N. *et al.* Receptor activator NF-kappaB ligand (RANKL) expression in synovial tissue from patients with rheumatoid arthritis, spondyloarthropathy, osteoarthritis, and from normal patients: semiquantitative and quantitative analysis. *Ann. Rheum. Dis.* **61,** 1047–1054 (2002).

13. Kannan, K., Ortmann, R. a & Kimpel, D. Animal models of rheumatoid arthritis and their relevance to human disease. *Pathophysiology* **12,** 167–181 (2005).

14. Bendele, A. Animal models of rheumatoid arthritis. *J. Musculoskelet. Neuronal Interact.* **1,** 377–385 (2001).

15. Schopf, L., Anderson, K. & Jaffee, B. Rat models of arthritis: Similarities, differences, advantages, and disadvantages in the identification of novel therapeutics. *vivo Model. Inflamm.* **I,** 1–34 (2006).

16. Webb, D. R. Animal models of human disease: inflammation. *Biochem. Pharmacol.* **87,** 121–130 (2014).

17. Joe, B. & Wilder, R. L. Animal models of rheumatoid arthritis. *Mol. Med. Today* **5,** 367–369 (1999).

18. Raggatt, L. J. & Partridge, N. C. Cellular and molecular mechanisms of bone remodeling. *J. Biol. Chem.* **285,** 25103–8 (2010).

19. Seeman, E. & Delmas, P. D. Bone quality-the material and structural basis of bone strength and fragility. *N. Engl. J. Med.* **354,** 2250–2261 (2006).

20. Hadjidakis, D. J. & Androulakis, I. I. Bone remodeling. *Ann. N. Y. Acad. Sci.* **1092,** 385–396 (2006).

21. Kini, U. & Nandeesh, B. N. *Radionuclide and Hybrid Bone Imaging*. Chapter 2: 29–55 (Springer Berlin Heidelberg, 2012). doi:10.1007/978-3-642-02400-9

22. Clarke, B. Normal bone anatomy and physiology. *Clin. J. Am. Soc. Nephrol.* **3 Suppl 3,** S131–S139 (2008).

23. Boskey, A. L. Bone composition: relationship to bone fragility and antiosteoporotic drug effects. *Bonekey Rep.* **2,** 1–11 (2013).

24. Kikuchi, M. Hydroxyapatite / Collagen Bone-Like Nanocomposite. *Biol. Pharm. Bull.* **36,** 1666–1669 (2013).

25. Ducy, P. The role of osteocalcin in the endocrine cross-talk between bone remodelling and energy metabolism. *Diabetologia* **54,** 1291–1297 (2011).

26. Hoang, Q. Q., Sicheri, F., Howard, A. J. & Yang, D. S. C. Bone recognition mechanism of porcine osteocalcin from crystal structure. *Nature* **425,** 977–980 (2003).

27. Balcerzak, M. *et al.* The roles of annexins and alkaline phosphatase in mineralization process. *Acta Biochim. Pol.* **50,** 1019–1038 (2003).

28. Milat, F. & Ng, K. W. Is Wnt signalling the final common pathway leading to bone formation? *Mol. Cell. Endocrinol.* **310,** 52–62 (2009).

29. Pérez-Sayáns, M., Somoza-Martín, J. M., Barros-Angueira, F., Rey, J. M. G. & García-García, A. RANK/RANKL/OPG role in distraction osteogenesis. *Oral Surg. Oral Med. Oral Pathol. Oral Radiol. Endod.* **109,** 679–686 (2010).

30. Takahashi, N., Maeda, K., Ishihara, A., Uehara, S. & Kobayashi, Y. Regulatory mechanism of osteoclastogenesis by RANKL and Wnt signals. *Front. Biosci.* **16,** 21–30 (2011).

31. W. Huang, S. Yang, J. Shao, Y. L. Signaling and transcriptional regulation in osteoblast commitment and differentiation. *Front. Biosci.* **12,** 3068–3092 (2007).

32. Zhang, R. *et al.* Bone Resorption by Osteoclasts. *Science (80-.).* **289,** 1504–1508 (2000).

33. Sims, N. a & Gooi, J. H. Bone remodeling: Multiple cellular interactions required for coupling of bone formation and resorption. *Semin. Cell Dev. Biol.* **19,** 444–451 (2008).

34. Ortuño, M. J., Susperregui, A. R. G., Artigas, N., Rosa, J. L. & Ventura, F. Osterix induces Col1a1 gene expression through binding to Sp1 sites in the bone enhancer and proximal promoter regions. *Bone* **52,** 548–556 (2013).

35. Neve, A., Corrado, A. & Cantatore, F. P. Osteocalcin: skeletal and extra-skeletal effects. *J. Cell. Physiol.* **228,** 1149–1153 (2013).

36. Kim, Y.-S., Paik, I.-Y., Rhie, Y.-J. & Suh, S.-H. Integrative physiology: Defined novel metabolic roles of osteocalcin. *J. Korean Med. Sci.* **25,** 985–991 (2010).

37. Rammelt, S. *et al.* Osteocalcin enhances bone remodeling around hydroxyapatite/collagen composites. *J. Biomed. Mater. Res. A* **73,** 284–294 (2005).

38. Rossini, M., Gatti, D. & Adami, S. Involvement of WNT/β-catenin signaling in the treatment of osteoporosis. *Calcif. Tissue Int.* **93,** 121–132 (2013).

39. Kobayashi, Y., Maeda, K. & Takahashi, N. Roles of Wnt signaling in bone formation and resorption. *Jpn. Dent. Sci. Rev.* **44,** 76–82 (2008).

40. Y. Wang, Y. Li, C. Paulson, J. Shao, X. Zhang, M. Wu, W. C. Wnt and the Wnt signaling pathway in bone development and disease. *J. Infect. Dis.* **19,** 379–407 (2014).

41. Future Medicine. No Title. *Futur. Oncol.* at <http://www.medscape.com/viewarticle/723850_4>

42. Diarra, D. *et al.* Dickkopf-1 is a master regulator of joint remodeling. *Nat. Med.* **13,** 156–163 (2007).

43. Power, J. *et al.* Sclerostin and the regulation of bone formation: Effects in hip osteoarthritis and femoral neck fracture. *J. Bone Miner. Res.* **25,** 1867–1876 (2010).

44. Tu, X. *et al.* Sost downregulation and local Wnt signaling are required for the osteogenic response to mechanical loading. *Bone* **50,** 209–217 (2012).

45. Pajevic, P. D. Recent Progress in Osteocyte Research. *Endocronology Metab.* **28,** 255–261 (2013).

46. Rochefort, G. Y. The osteocyte as a therapeutic target in the treatment of osteoporosis. *Ther. Adv. Musculoskelet. Dis.* **6,** 79–91 (2014).

47. Sims, N. a & Martin, T. J. Coupling the activities of bone formation and resorption: a multitude of signals within the basic multicellular unit. *Bonekey Rep.* **3,** 1–10 (2014).

48. Cappariello, A., Maurizi, A., Veeriah, V. & Teti, A. The Great Beauty of the osteoclast. *Arch. Biochem. Biophys.* **558,** 70–78 (2014).

49. Coiffier, G. *et al.* Common bone turnover markers in rheumatoid arthritis and ankylosing spondylitis: a literature review. *Joint. Bone. Spine* **80,** 250–257 (2013).

50. Vasikaran, S. *et al.* Markers of bone turnover for the prediction of fracture risk and monitoring of osteoporosis treatment: a need for international reference standards. *Osteoporos. Int.* **22,** 391–420 (2011).

51. Caetano-Lopes, J. *et al.* Rheumatoid Arthritis Bone Fragility Is Associated With Upregulation of IL17 and DKK1 Gene Expression. *Clin. Rev. Allergy Immunol.* **47,** 38–45 (2013).

52. Matzelle, M. M. *et al.* Resolution of inflammation induces osteoblast function and regulates the Wnt signaling pathway. *Arthritis Rheum.* **64,** 1540–1550 (2012).

53. Aletaha, D. *et al.* 2010 Rheumatoid arthritis classification criteria: An American College of Rheumatology/European League Against Rheumatism collaborative initiative. *Arthritis Rheum.* **62,** 2569–2581 (2010).

54. Cascão, R., Vidal, B. & Raquel, H. Potent Anti-Inflammatory and Antiproliferative Effects of Gambogic Acid in a Rat Model of Antigen-Induced Arthritis. *Mediat. …* **2014,** 195327 (2014).

55. Peckham, M. The histology guide - What is H&E? (2003). at <http://histology.leeds.ac.uk/what-is-histology/H_and_E.php>

56. World, I. Introduction to Immunohistochemistry. (2003). at <http://www.ihcworld.com/_intro/intro.htm>

57. Vidal, B. *et al.* Bone histomorphometry revisited. *Acta Reumatol. Port.* **37,** 294–300 (2012).

58. Doube, M. *et al.* BoneJ: Free and extensible bone image analysis in ImageJ. *Bone* **47,** 1076–1079 (2010).

59. Schneider, C. A., Rasband, W. S. & Eliceiri, K. W. NIH Image to ImageJ: 25 years of image analysis. *Nat. Methods* **9,** 671–675 (2012).

60. Abràmoff, M. D., Magalhães, P. J. & Ram, S. J. Image processing with imageJ. *Biophotonics Int.* **11,** 36–41 (2004).

61. Abdulghani, S., Caetano-Lopes, J., Canhão, H. & Fonseca, J. E. Biomechanical effects of inflammatory diseases on bone-rheumatoid arthritis as a paradigm. *Autoimmun. Rev.* **8,** 668–671 (2009).

62. Caetano-Lopes, J. Effect of inflammation on bone biological, structural and mechanical behaviour. (2011).

63. Caetano-Lopes, J. *et al.* Chronic arthritis directly induces quantitative and qualitative bone disturbances leading to compromised biomechanical properties. *Clin. Exp. Rheumatol.* **27,** 475–482 (2009).

64. Heid, C. a, Stevens, J., Livak, K. J. & Williams, P. M. Real time quantitative PCR. *Genome Res.* **6,** 986–994 (1996).

65. Wong, M. L. & Medrano, J. F. Real-time PCR for mRNA quantitation. *Biotechniques* **39,** 75–85 (2005).

66. Roche Diagnostics. Universal ProbeLibrary Assay Design Center. (1996). at <http://qpcr.probefinder.com/roche3.html>

67. Caetano-Lopes, J. *et al.* Upregulation of inflammatory genes and downregulation of sclerostin gene expression are key elements in the early phase of fragility fracture healing. *PLoS One* **6,** 1–7 (2011).

68. Vossenaar, E. R. & van Venrooij, W. J. Anti-CCP antibodies, a highly specific marker for (early) rheumatoid arthritis. *Clin. Appl. Immunol. Rev.* **4,** 239–262 (2004).

69. Song, Y. W. & Kang, E. H. Autoantibodies in rheumatoid arthritis: rheumatoid factors and anticitrullinated protein antibodies. *QJM* **103,** 139–146 (2010).

70. Favalli, E. G., Biggioggero, M. & Meroni, P. L. Methotrexate for the treatment of rheumatoid arthritis in the biologic era: Still an “anchor” drug? *Autoimmun. Rev.* (2014). doi:10.1016/j.autrev.2014.08.026

71. Wisłowska, M., Jakubicz, D., Stępień, K. & Cicha, M. Serum concentrations of formation (PINP) and resorption (Ctx) bone turnover markers in rheumatoid arthritis. *Rheumatol. Int.* **29,** 1403–1409 (2009).

72. Brown, S. J., Pollintine, P., Powell, D. E., Davie, M. W. J. & Sharp, C. A. Regional differences in mechanical and material properties of femoral head cancellous bone in health and osteoarthritis. *Calcif. Tissue Int.* **71,** 227–234 (2002).

73. Rodrigues, A. *et al.* Evaluation of bone mechanical strenght and fracture risk assessment (Frax) in patients with hip joint

replacement surgery. *Acta Reum. Port.* **34,** 504–510 (2009).

74. Xu, S., Wang, Y., Lu, J. & Xu, J. Osteoprotegerin and RANKL in the pathogenesis of rheumatoid arthritis-induced osteoporosis. *Rheumatol. Int.* **32,** 3397–3403 (2012).

75. Kotake, S. *et al.* Activated human T cells directly induce osteoclastogenesis from human monocytes: possible role of T cells in bone destruction in rheumatoid arthritis patients. *Arthritis Rheum.* **44,** 1003–1012 (2001).

76. Skalska, U., Prochorec-Sobieszek, M. & Kontny, E. Osteoblastic potential of infrapatellar fat pad-derived mesenchymal stem cells from rheumatoid arthritis and osteoarthritis patients. *Int. J. Rheum. Dis.* (2014). doi:10.1111/1756-185X.12368

77. Imai, K. *et al.* Differential expression of WNTs and FRPs in the synovium of rheumatoid arthritis and osteoarthritis. *Biochem. Biophys. Res. Commun.* **345,** 1615–1620 (2006).

78. Ijiri, K. *et al.* Differential expression patterns of secreted frizzled related protein genes in synovial cells from patients with arthritis. *J. Rheumatol.* **29,** 2266–2270 (2002).

79. Appel, H. *et al.* Altered skeletal expression of sclerostin and its link to radiographic progression in ankylosing spondylitis. *Arthritis Rheum.* **60,** 3257–3262 (2009).

80. NIH. Bone Mass Measurement: What the Numbers Mean. (2012). at <http://www.niams.nih.gov/Health_Info/Bone/Bone_Health/bone_mass_measure.pdf>

81. Xu, X., Shen, L., Yang, Y., Lu, F., Zhu, R., Shuai, B., Li, C. Wu, M. Serum sclerostin levels associated with lumbar spine bone mineral osteoporosis. *Chin. Med. J. (Engl).* **126,** 2480–2484 (2013).

82. Patsch, J. M. *et al.* Trabecular bone microstructure and local gene expression in iliac crest biopsies of men with idiopathic osteoporosis. *J. Bone Miner. Res.* **26,** 1584–1592 (2011).

83. D'Amelio, P. *et al.* Bone and bone marrow pro-osteoclastogenic cytokines are up-regulated in osteoporosis fragility fractures. *Osteoporos. Int.* **22,** 2869–2877 (2011).

84. Dovjak, P. *et al.* Serum Levels of Sclerostin and Dickkopf-1: Effects of Age, Gender and Fracture Status. *Gerontology* **60,** 493–501 (2014).

85. Montagnani, A. Bone anabolics in osteoporosis: Actuality and perspectives. *World J. Orthop.* **5,** 247–254 (2014).

86. Cai, X. *et al.* The comparative study of Sprague-Dawley and Lewis rats in adjuvant-induced arthritis. *Naunyn. Schmiedebergs. Arch. Pharmacol.* **373,** 140–147 (2006).

87. Noguchi, M., Kimoto, A., Sasamata, M. & Miyata, K. Micro-CT imaging analysis for the effect of celecoxib, a cyclooxygenase-2 inhibitor, on inflammatory bone destruction in adjuvant arthritis rats. *J. Bone Miner. Metab.* **26,** 461–468 (2008).

88. Nanjundaiah SM, Stains JP, M. K. Kinetics and interplay of mediators of inflammation-induced bone damage in the course of adjuvant arthritis. *Int. J. Immunopathol. Pharmacol.* **26,** 37–48 (2013).

89. Osterman, T. *et al.* Slow-release clodronate in prevention of inflammation and bone loss associated with adjuvant arthritis. *J. Pharmacol. Exp. Ther.* **280,** 1001–1007 (1997).

90. Kishimoto, Y. *et al.* Gene expression relevant to osteoclastogenesis in the synovium and bone marrow of mature rats with collagen-induced arthritis. *Rheumatology (Oxford).* **43,** 1496–1503 (2004).

91. Ho, T.-Y., Santora, K., Chen, J. C., Frankshun, A.-L. & Bagnell, C. a. Effects of relaxin and estrogens on bone remodeling markers, receptor activator of NF-kB ligand (RANKL) and osteoprotegerin (OPG), in rat adjuvant-induced arthritis. *Bone* **48,** 1346–53 (2011).

92. Engdahl, C. *et al.* Periarticular bone loss in antigen-induced arthritis. *Arthritis Rheum.* **65,** 2857–2865 (2013).

Anex 1

Human primers

Gene symbol	Gene name	GenBank number	Product length (bp)	Primer sequences
PMM1	Phosphomannomutase 1 (Housekeeping)	NM_002676	96	F:GAATGGCATGCTGAACATCTC R:TCCCGGATCTTCTCTTTCTTG
ALP	Bone Alkaline phosphatase	NM_000478.3	74	F:GCGCAGGATTGGAACATC R:CCCAAGACCTGCTTTATCCC
COL1A1	Collagen type I alpha 1	NM_00085313.3	129	F:ACGAAGACATCCCACCAATC R:AGATCACGTCATCGCACAAC
DKK1	Dickkopf protein 1	NM_012242.2	120	F: CAGGCGTGCAAATCTGTCT R: AATGATTTTGATCAGAAGACACACATA
DKK2	Dickkopf protein 2	NM_014421	72	F: GGCAGTAAGAAGGGCAAAAA R: CCTCCCAACTTCTTCACACTCCT
LRP5	Low-Density Lipoprotein Receptor-Related Protein 5	NM_002335.2	60	F: GAACATCAAGCGAGCCAAG R: TGGCTCAGAGAGGTCAAAACA
LRP6	Low-Density Lipoprotein Receptor-Related Protein 6	NM_002336.2	64	F: ATCCGAAAGGCACAAGAAGA R: GACTCGGAACTGAGCTCACAA
OCN	Osteocalcin	NM_199173	198	F:CCAGGCAGGTGCGAAG R:TCAGCCAACTCGTCACAGTC
OPG	Osteoprotegerin	NM_002546	185	F:CGCTCGTGTTTCTGGACAT R:GTAGTGGTCAGGGCAAGGG
OSX	Osterix	NM_152860.1	91	F:CCCTGCTTGAGGAGGAAGTT R:GTAAAGGGGGCTGGATAAGC
RANKL	Receptor activator of nuclear factor kappa-B ligand	NM_003701	116	F:AGAGAAAGCGATGGTGGATG R:TATGGGAACCAGATGGGATG
RUNX2	Runt-related transcription factor 2	NM_004348	193	F:CGGAATGCCTCTGCTGTTA R:TCTGTCTGTGCCTTCTGGGT
SEMA 3A	Semaphorin 3A	NM_006080.2	65	F:TGAAATTGGACATCATCCTGAG R:GGCCGTTTTCAAAATGTGAG
SFRP1	Secreted frizzled-related protein 1	NM_003012.4	75	F:GCTGGAGCACGAGACCAT R:TGGCAGTTCTTGTTGAGCA
SOST	Sclerostin	NM_025237	196	F:AGACCAAAGACGTGTCCGAG R:GGGATGCAGCGGAAGTC
WIF1	WNT inhibitory factor 1	NM_007191	72	F: CCAGGGAGACCTCTGTTCAA R: TTGGGTTCATGGCAGGTT
WNT10B	Wingless-type MMTV integration site family member 10B	NM_003394	107	F: GCGAATCCACAACAACAGG R: TCCAGCATGTCTTGAACTGG

Rat primers

Gene symbol	Gene name	GenBank number	Product length (bp)	Primer sequences
RPS29	Ribossomal protein S29 (Housekeeping)	NM_012876.1	109	F:TCCTTTTTCCTCCTTGGGCG R:TTAGAGCAGACGCGGCAAGA
CTSK	Cathepsin K	NM_031560.2	73	F: GGGAGACATGACCAGCGAAG R: ACTGAAGGAACGCGAAGGTG
LRP6	Low density lipoprotein receptor-related proein 6	NM_001107892.1	145	F:GCAAAGATGGTGCCACTGAA R:TCCACGGGGTCGTAGTCTAT
OCN	Osteocalcin	NM_013414.1	91	F: TCAACAATGGACTTGGAGCCC R: AGCTCGTCACAATTGGGGTT
OPG	Osteoprotegerin	NM_012870.2	108	F: CTCACTTGGCCTCCTGCTAA R: TCGCACAGGGTGACATCTAT
RANKL	Receptor activator of nuclear factor kappa-B ligand	NM_057149.1	98	F: CGAGCGCAGATGGATCCTA R:AGTGCTTCTGTGTCTTCGC
WIF-1	WNT inhibitory factor 1	NM_053738.1	95	F: GGCATCAGTTGTTCAAGTTGGTTTC R: TGCCTTCAGAATTCATGACAATCAC
WNT10B	Wingless-type MMTV integration site family member 10B	NM_001108111.1	102	F: GTTCAGTCGGGCTCTAAGCA R:TTACTCAAGCCGGACAGGGT